AD-A057 423 SPACE DATA CORP TEMPE AZ F/G 4/1
ROCKETBORNE OZONESONDE UTILIZING CHEMILUMINESCENCE TO MEASURE A--ETC(U)
MAY 78 B BOLLERMANN, F HAYO DAAD07-75-C-0103
UNCLASSIFIED SDC-TM-1427 ASL-CR-78-0103-1 NL

| OF |
AD
A057423

END
DATE
FILMED
9-78
DDC

ASL-CR-78-0103-1

LEVEL II

AD
Reports Control Symbol
OSD-1366

ROCKETBORNE OZONESONDE UTILIZING CHEMILUMINESCENCE TO MEASURE ATMOSPHERIC OZONE

MAY 1978

Prepared by

Bruce Bollermann
Frank Hayo
Space Data Corporation
Tempe, Arizona 85282

UNDER CONTRACT DAAD07-75-C-0103
Contract Monitor: Jagir S. Randhawa

US Army Electronics Research and Development Command
Atmospheric Sciences Laboratory
White Sands Missile Range, N.M. 88002

NOTICES

Disclaimers

The findings in this report are not to be construed as an official Department of the Army position, unless so designated by other authorized documents.

The citation of trade names and names of manufacturers in this report is not to be construed as official Government indorsement or approval of commercial products or services referenced herein.

Disposition

Destroy this report when it is no longer needed. Do not return it to the originator.

SECURITY CLASSIFICATION OF THIS PAGE *(When Data Entered)*

REPORT DOCUMENTATION PAGE

READ INSTRUCTIONS BEFORE COMPLETING FORM

1. REPORT NUMBER: ASL-CR-78-0103-1	2. GOVT ACCESSION NO.
3. RECIPIENT'S CATALOG NUMBER	
4. TITLE *(and Subtitle)*: ROCKETBORNE OZONESONDE UTILIZING CHEMILUMINESCENCE TO MEASURE ATMOSPHERIC OZONE	5. TYPE OF REPORT & PERIOD COVERED: Technical Report
	6. PERFORMING ORG. REPORT NUMBER: SDC-TM-1427
7. AUTHOR(s): Bruce Bollermann, Frank Hayo	8. CONTRACT OR GRANT NUMBER(s): DAAD07-75-C-0103
9. PERFORMING ORGANIZATION NAME AND ADDRESS: Space Data Corporation, Tempe, AZ 85282	10. PROGRAM ELEMENT, PROJECT, TASK AREA & WORK UNIT NUMBERS: Task No. IT765020D127
11. CONTROLLING OFFICE NAME AND ADDRESS: US Army Electronics Research and Development Command, Adelphi, MD 20783	12. REPORT DATE: May 1978 13. NUMBER OF PAGES: 72
14. MONITORING AGENCY NAME & ADDRESS *(if different from Controlling Office)*: Atmospheric Sciences Laboratory, White Sands Missile Range, NM 88002	15. SECURITY CLASS. *(of this report)*: UNCLASSIFIED 15a. DECLASSIFICATION/DOWNGRADING SCHEDULE

16. DISTRIBUTION STATEMENT *(of this Report)*

Approved for public release; distribution unlimited.

17. DISTRIBUTION STATEMENT *(of the abstract entered in Block 20, if different from Report)*

18. SUPPLEMENTARY NOTES

Contract Monitor: Jagir S. Randhawa

19. KEY WORDS *(Continue on reverse side if necessary and identify by block number)*

Ozone
Super Loki
Chemiluminescent
Sensor
Mesosphere
Stratosphere

20. ABSTRACT *(Continue on reverse side if necessary and identify by block number)*

A chemilumiscent ozone sensor capable of measuring ozone concentration in the lower mesosphere and stratosphere has been developed. It is deployed with a small meteorological rocket (super Loki) of 5.4 cm diameter, at an altitude of 75 km and descends on a 2.1 meter STARUTE parachute. The sensor incorporates a new aerodynamic air sampling system which increases the flow of air over the detector to make possible the accurate measurement of ozone in the upper atmosphere. Calibration of the detector under simulated flight conditions as well

next page

DD FORM 1 JAN 73 1473 EDITION OF 1 NOV 65 IS OBSOLETE

SECURITY CLASSIFICATION OF THIS PAGE *(When Data Entered)*

20. ABSTRACT (cont)

as its dependence upon the flow rate are described. Test results obtained at White Sands Missile Range (32°N) are compared to those of other experimenters.

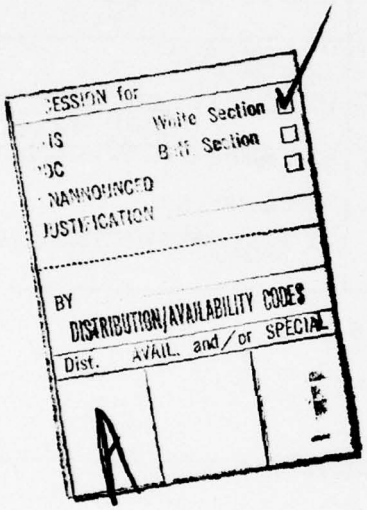

TABLE OF CONTENTS

1.0 INTRODUCTION

Scientists are aware and the general public is becoming more and more aware that life on earth is possible only because the atmospheric ozone layer exists.[1] Ultraviolet light from the sun is absorbed by the ozone layer, preventing ultraviolet rays in quantities dangerous to human existence from reaching the earth.[2] Were the ozone layer to be destroyed, there would be no such safety shield protecting life on earth.

Medical experts may have linked excessive ultraviolet light exposure to cancer and are justifiably concerned that even partial deterioration of the ozone layer would allow more ultraviolet light to penetrate to the earth's surface, increasing in number the victims of cancer.[3]

We know that ozone is very unstable and that it disassociates readily.[4] The ozone "layer" is really an ozone equilibrium, a balance between ozone being created and destroyed. Atmospheric contaminants such as may be released from aerosol cans or jet engine exhaust may rise high enough to reach the ozone layer.[5] If they do, the ozone equilibrium could be upset, with only negative consequences.

The only way to "keep an eye" on the ozone layer is to measure it, and the best way to measure it at altitudes higher than 30 km is via sounding rockets.

An ideal way to measure the ozone layer is to incorporate an ozonesonde that is compatible with meteorological rockets that are currently being launched

daily from facilities around the world. Such a system, if feasible, would provide a necessary safety measure at minimal added costs.

The detection method is to use a sensor disk coated with a Rhodamine B solution, which, when contacted by ozone, results in a light-emitting chemical reaction (a chemiluminescent reaction). The measurement technique is to measure the intensity of the light emitted due to the ozone-Rhodamine B reaction. Theoretically, the greater the intensity, the more ozone there is.

The detection system must be designed so that the light meter measures only light emitted due to the chemiluminescence. Extraneous sunlight, if visible by the light meter, would give false ozone readings. Therefore, the ozonesonde design must allow flow of a representative air sample while simultaneously blocking out stray light. One proposed design is shown in Figures 1.1 and 1.2.

The purpose of the research effort described in this report was to define the quantitative relationship between the intensity of the emitted light and the ozone concentration and to reveal and (if possible) solve other problems introduced as a result of the research effort.

Consistency and repeatability of results were investigated during Sensitivity Tests. Several questions arose in this area, none of which precluded the chemiluminescent technique for measuring ozone.

Detector output versus ozone concentration as functions of flow rate and pressure were investigated, though on a limited basis due to economic constraints

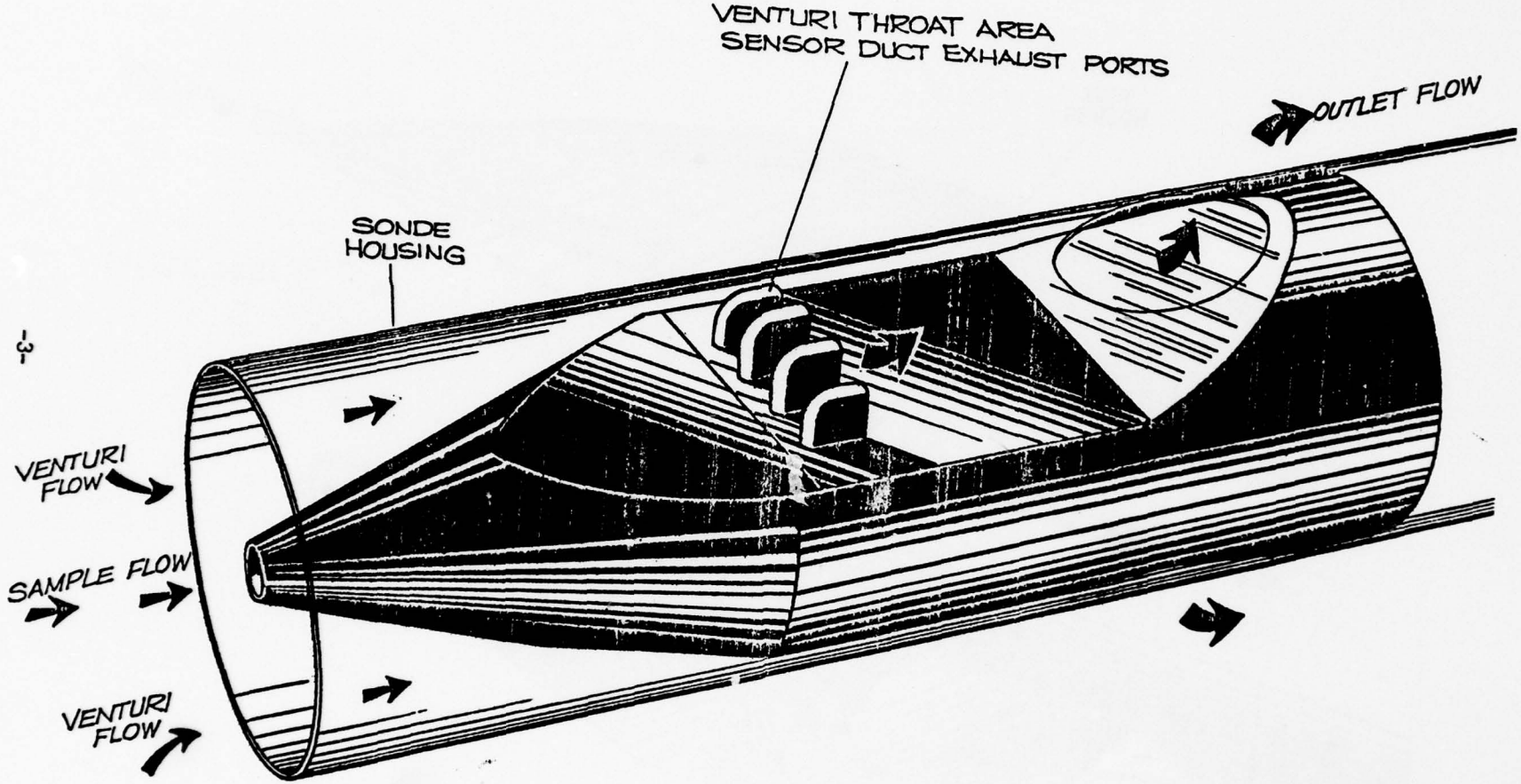

FIGURE 1.1
OZONESONDE AIR SAMPLING
PROBE CONFIGURATION

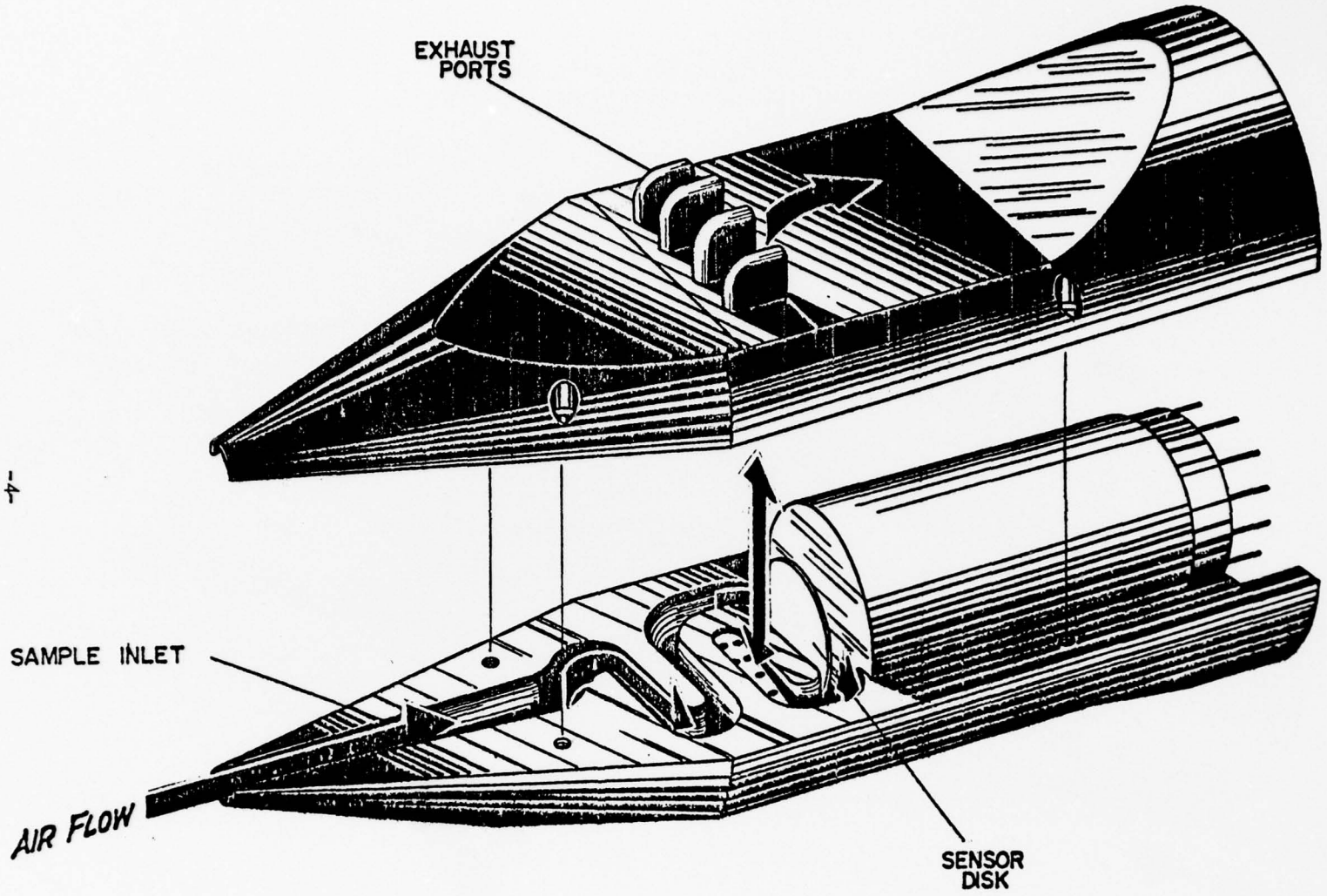

FIGURE 1.2
OZONESONDE AIR SAMPLING
PROBE CONFIGURATION

of the contract. These tests revealed the importance of flow rate on the data reduction technique. Because in-flight flow metering is too expensive to be practical, flow rates through the ozonesonde ducts must be calculated. (See SDC TM-1414.) To verify flow rate calculations, blowdown tests were conducted.

Inlet losses were investigated, but they were found to be insignificant within the range of tests conducted.

Finally, vibration tests were conducted in order to determine whether vibrations experienced during flight would be sufficiently forceful to cause the sensor material to flake off, resulting in decreased sensitivity. They were not.

As a result of these tests, the conclusion drawn is that the rocketborne ozonesonde employing the chemiluminescent technique for measuring atmospheric ozone is feasible. The following sections describe test results and define the atmospheric ozone data reduction technique.

2.0 SENSITIVITY TESTS

2.1 Introduction

The proposed technique for measuring atmospheric ozone incorporates a photomultiplier to measure the light emitted as a result of a chemiluminescent reaction between ozone and Rhodamine B, a solution of which is coated on the ozonesonde sensor disk surface. Theoretically, there is a measurable relationship between the amount of ozone reacting with Rhodamine B and the intensity of the resulting emitted light.

The purpose of the Sensitivity Tests was to study the relationships between ozone concentration and detector (photomultiplier) output. Clearly, consistent and repeatable results (per individual disks) are mandatory if ozone measurements are to be accurate and valid. To facilitate repeatability, an ozone generator that would enable known amounts of ozone to be created at repeatable rates was constructed. Ozone is created by bombarding a mixture of oxygen and nitrogen gases with ultraviolet light – as is done in the atmosphere, where the sun provides the ultraviolet light (UV) source. The more UV there is, the more ozone is generated, and the relationship is a direct proportion. What the ozone generator does is uncover/cover a UV lamp at a constant rate, such that more/less ozone is created. A Dasibi ozone monitor measures the amount of ozone created, and a strip chart recorder can be (and was) used to record the Dasibi ozone concentration measurements and the photomultiplier output. Figure 2.1 is a schematic of the test setup.

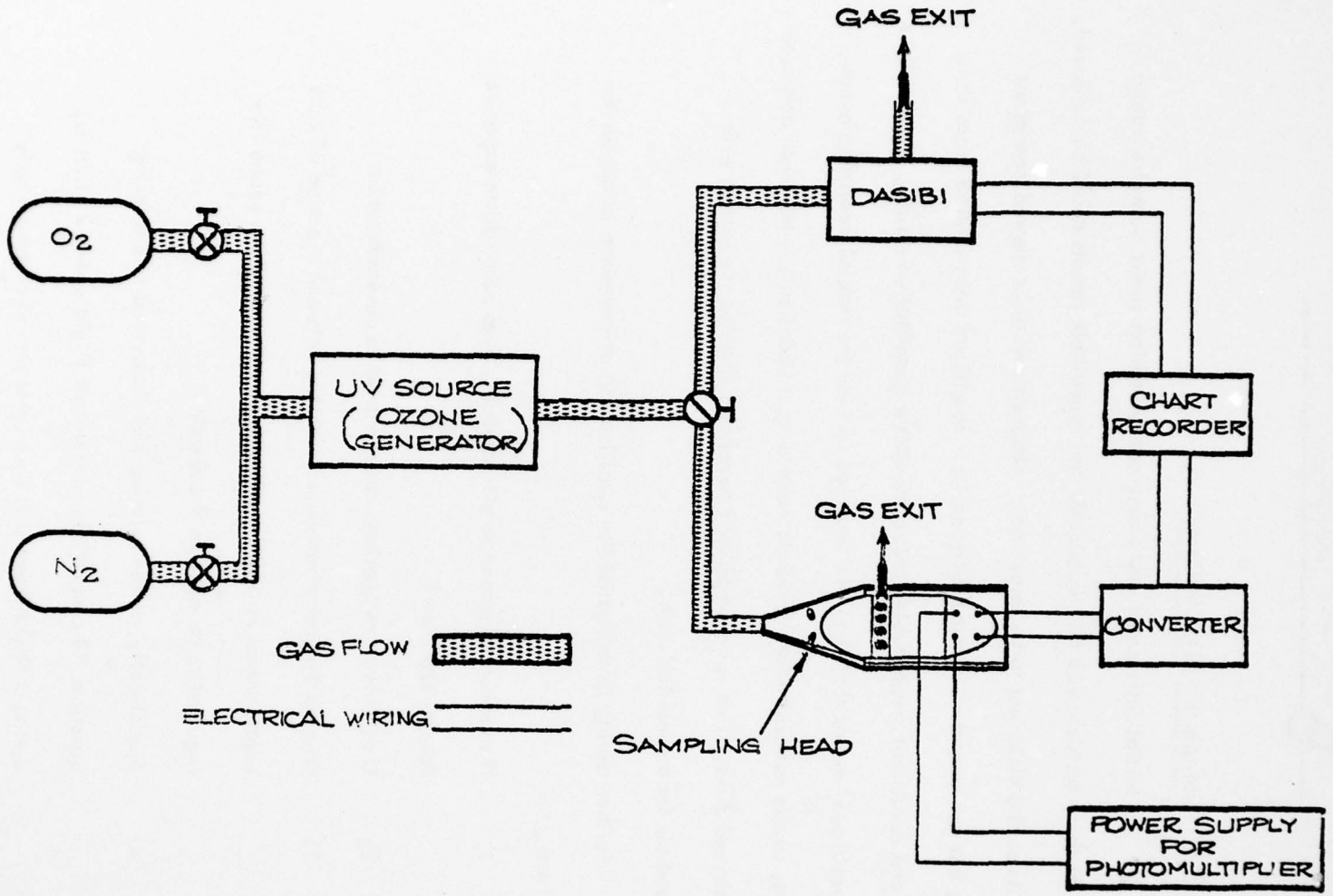

FIGURE 2.1, TEST SETUP

2.2 Results and Observations

Initial tests monitored ozone concentration versus detector output. Results of these tests showed that consistent and repeatable results could be achieved, but to do so the disks had to be sensitized. Unsensitized disks showed consistent trends, but not consistent quantitative results. Sensitized disks showed consistent trends and consistent, repeatable, and predictable quantitative results. To say disks are "sensitized" means that they are "warmed up" for the task of measuring ozone. That is, ozone concentration versus detector output stabilization has been achieved in sensitized disks. This is accomplished merely by flushing the system with ozonized air for a specified time.

Further testing investigated the sensitization phenomenon to answer the questions:

1) If exposure to ozone sensitizes disks, does zero ozone exposure desensitize them?
2) If so, what time periods are involved in desensitization?
3) What is the quantitative relationship between a period of zero ozone exposure and the subsequent and immediate ozone flux required to resensitize the disks?
4) Specifically, is the relationship discovered in answering question #3 compatible with actual flight events? That is, during a flight there will be a brief period of zero ozone exposure. If that period is such that significant disk

desensitization occurs, how much subsequent ozone exposure is required to resensitize the disk? Is the amount of ozone present at high altitudes sufficient in quantity to accommodate disk resensitization at flow rates expected during flight?

To answer these questions, the same test setup as shown in Figure 2.1 was used. The test procedure was to sensitize the disks by flushing with ozone of 1 part per million by volume (ppmV) concentration for ten minutes at 1 liter/minute flow rate. A cycle run was made to measure ozone concentration versus photomultiplier output for a sensitized disk. (During initial tests of this kind two more cycles were conducted and the subsequent, repeatable results proved the disks to be sensitized.)

The disk then sat idle for a specified time, after which cycle runs were made. Data taken after an idle period were compared with pre-idle data, and the difference showed the effect of zero ozone exposure for that idle period.

Results were that periods of zero ozone exposure did cause disk desensitization, resulting in an inconsistent overshoot phenomenon. That is, desensitized disks exhibited a greater photomultiplier response than sensitized disks. When the ozone concentration was held constant, the desensitized disk's photomultiplier response decreased until stabilization (resensitization) occurred. The time required for stabilization varied, depending upon the degree of desensitization and the ozone flux through the sensor duct during resensititzation.

Figure 2.2 exhibits the overshoot phenomenon observed in desensitized disks. The particular disk shown in Figure 2.2 was left idle for fifteen minutes. Figure 2.3 shows the same disk's photomultiplier response after an idle period of two minutes.

Comparison of Figures 2.2 and 2.3 shows that the longer the idle period of zero ozone exposure, the stronger the disk desensitization, the greater the overshoot and the longer the period required to resensitize the disk.

The effect of overshoot is to flatten out the photomultiplier response curve. In isolated cases, the overshoot effect even reversed the slope of the photomultiplier response curve! Clearly, if photomultiplier response is to be used to show the amount of ozone present, the overshoot phenomenon cannot be present. That is, disks must be sensitized.

Figure 2.4 shows the ozone concentration versus photomultiplier output for a sensitized disk. Note how, after an initial bend, the response is relatively linear and is therefore very useful for measuring ozone.

Figure 2.5 shows the same disk after an idle period of 15 minutes. Note how the photomultiplier response overshoots the reading of the same disk when sensitized for the same early ozone concentrations. As the disk becomes more exposed to ozone, it becomes resensitized, and if the ozone concentration were held constant, the photomultiplier response would decrease until stable. But the ozone concentration is increasing, so the photomultiplier response is also increasing, although its rate of increase is decreasing and will continue to decrease until the disk is resensitized.

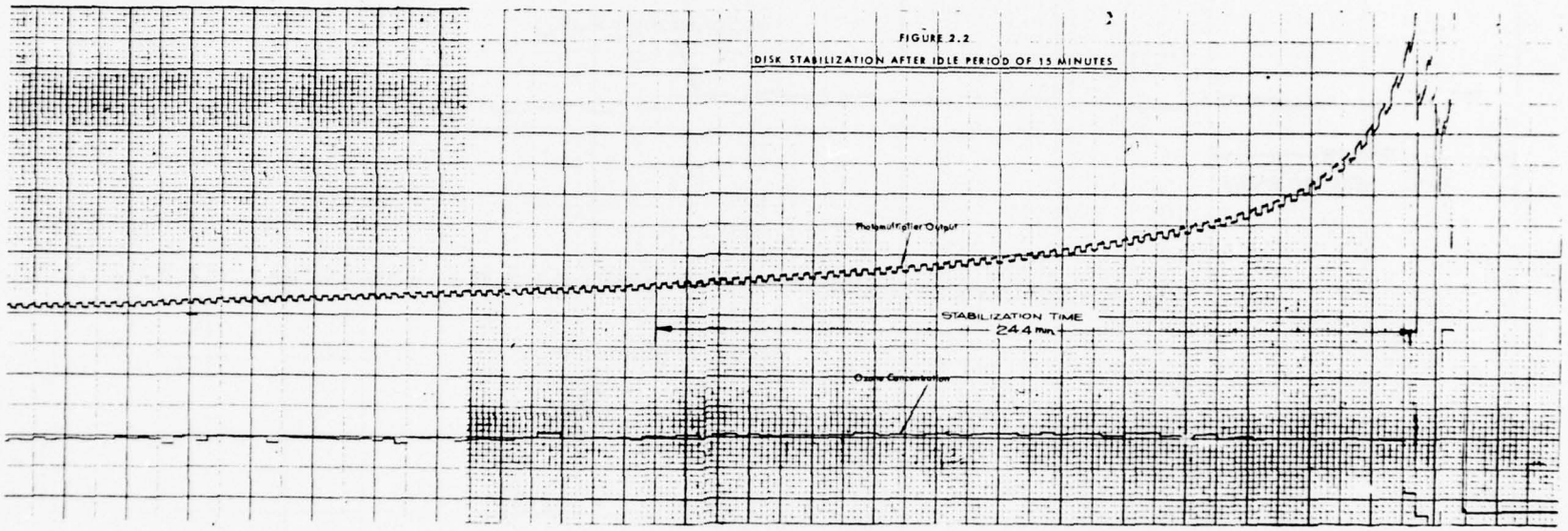

FIGURE 2.2
DISK STABILIZATION AFTER IDLE PERIOD OF 15 MINUTES

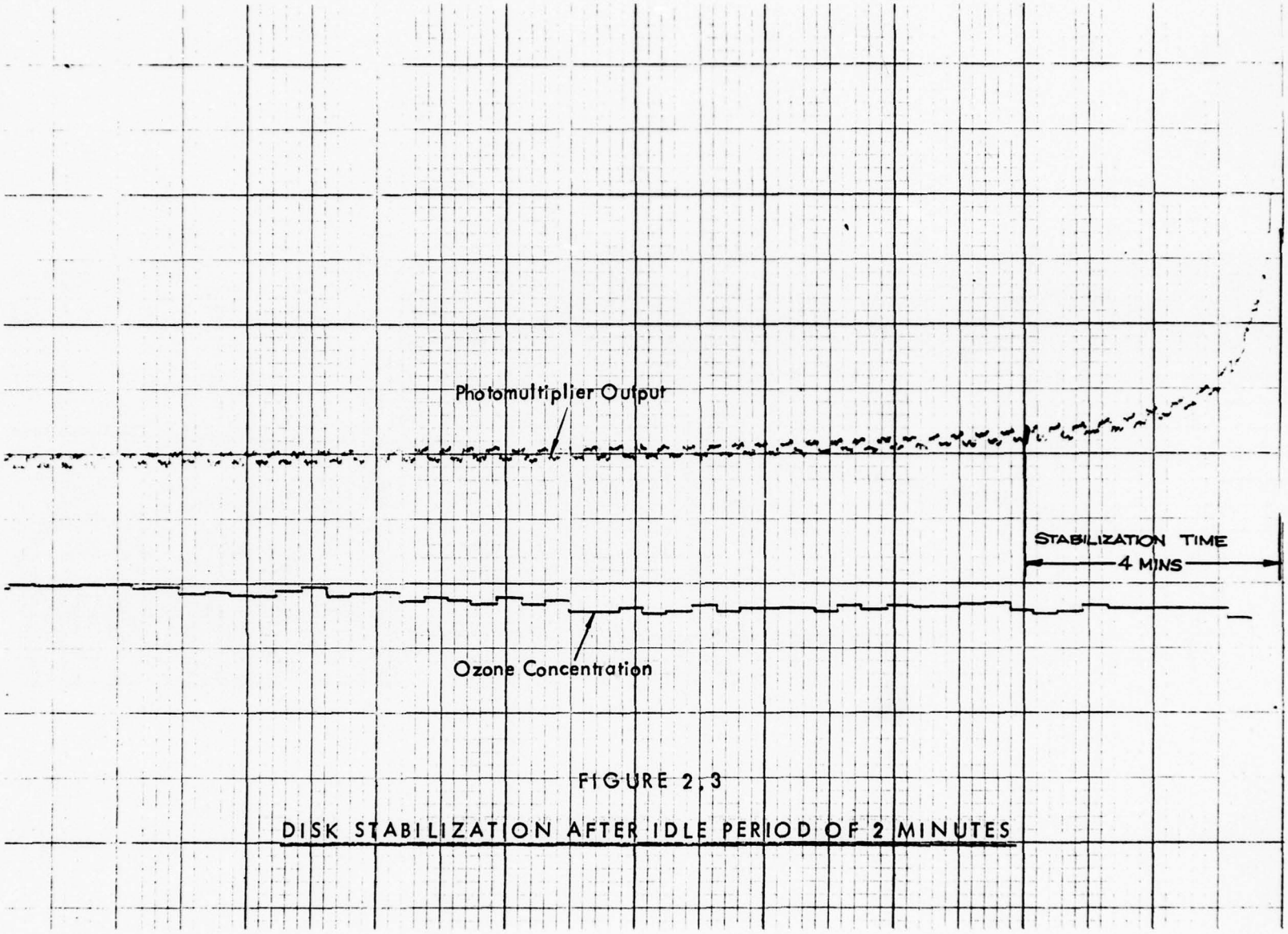

FIGURE 2.3

DISK STABILIZATION AFTER IDLE PERIOD OF 2 MINUTES

FIGURE 2.4

SENSITIZED DISK'S DETECTOR OUTPUT
VERSUS OZONE CONCENTRATION

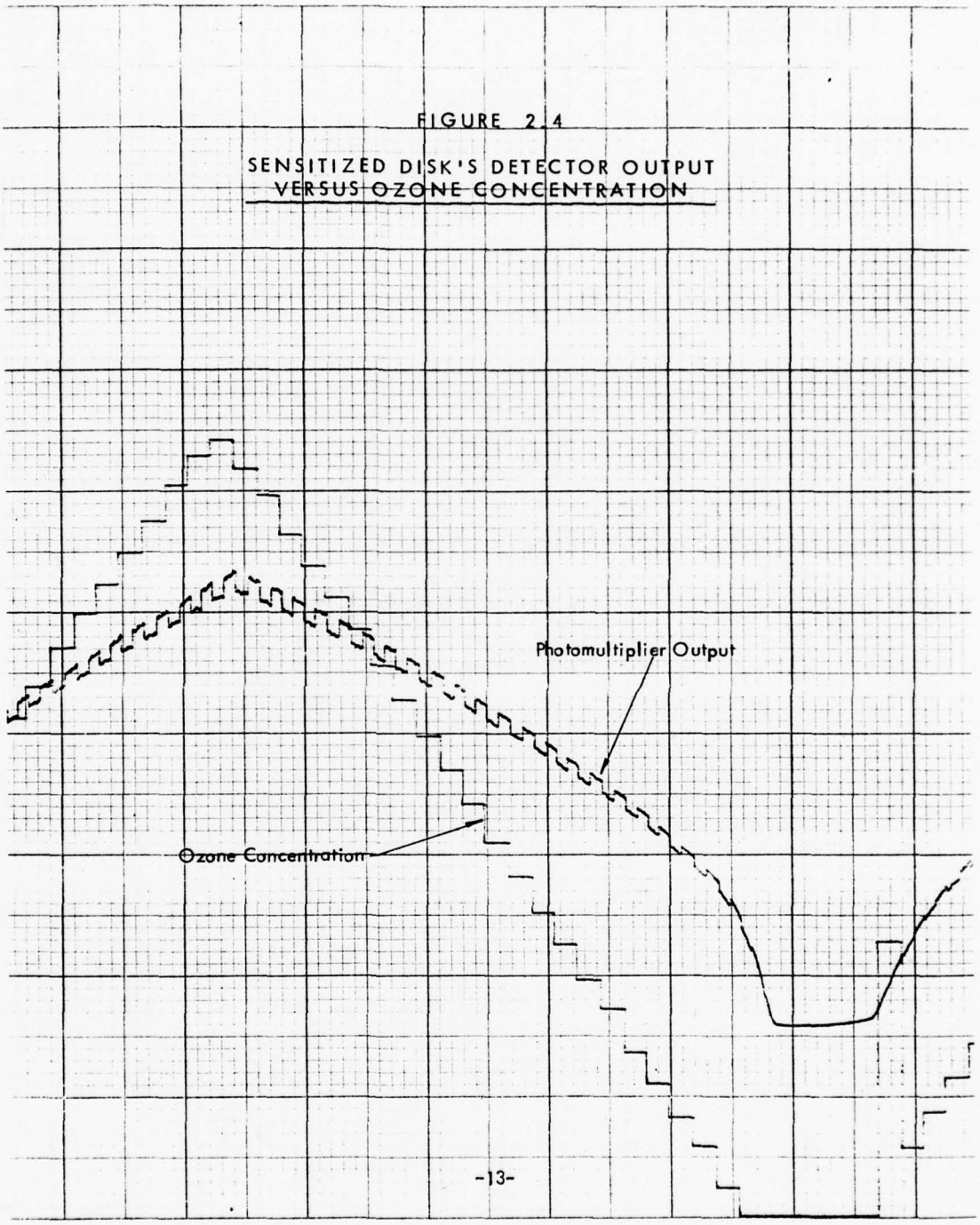

FIGURE 2.5

DESENSITIZED DISK'S
DETECTOR OUTPUT VERSUS OZONE CONCENTRATION

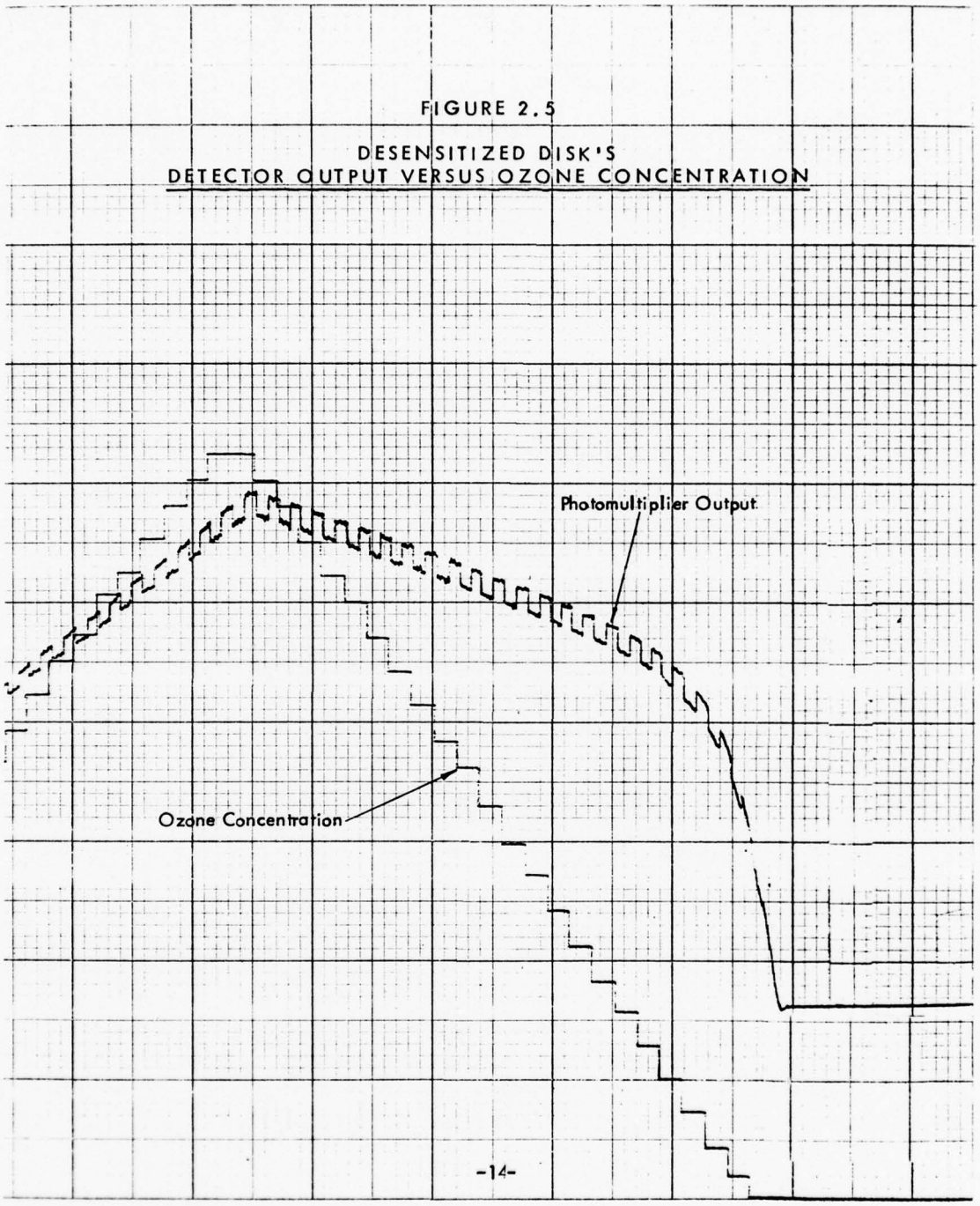

Figure 2.6 shows an example of a drastic overshoot in photomultiplier response. Clearly, this response is unacceptable for ozone measurements. For this case, there is no way to relate photomultiplier response to a specific ozone concentration.

When the disk of Figure 2.6 is sensitized, its response curve is stable, as shown in Figure 2.7. Clearly, the disk – when sensitized – is useful for measuring ozone.

Thus, the answers to the first two questions are:

1) Periods of zero ozone exposure do result in disk desensitization, and

2) Idle periods as brief as two minutes can cause measurable disk desensitization.

Since the time between liftoff and the start of ozone measurements is on the order of two minutes, measurable disk desensitization can occur, even if disks are continuously flushed with ozone until liftoff.

Test procedures to measure resensitization versus desensitization times were as follows:

1) Disks were fully sensitized.

2) Disks underwent a specified idle period.

3) Disks were flushed with ozone at constant concentrations, the stabilization was recorded and the stabilization time was measured.

Results of these tests are shown in Table 2.1.

FIGURE 2.6

DESENSITIZED DISK
EXHIBITING DRASTIC OVERSHOOT PHENOMENON

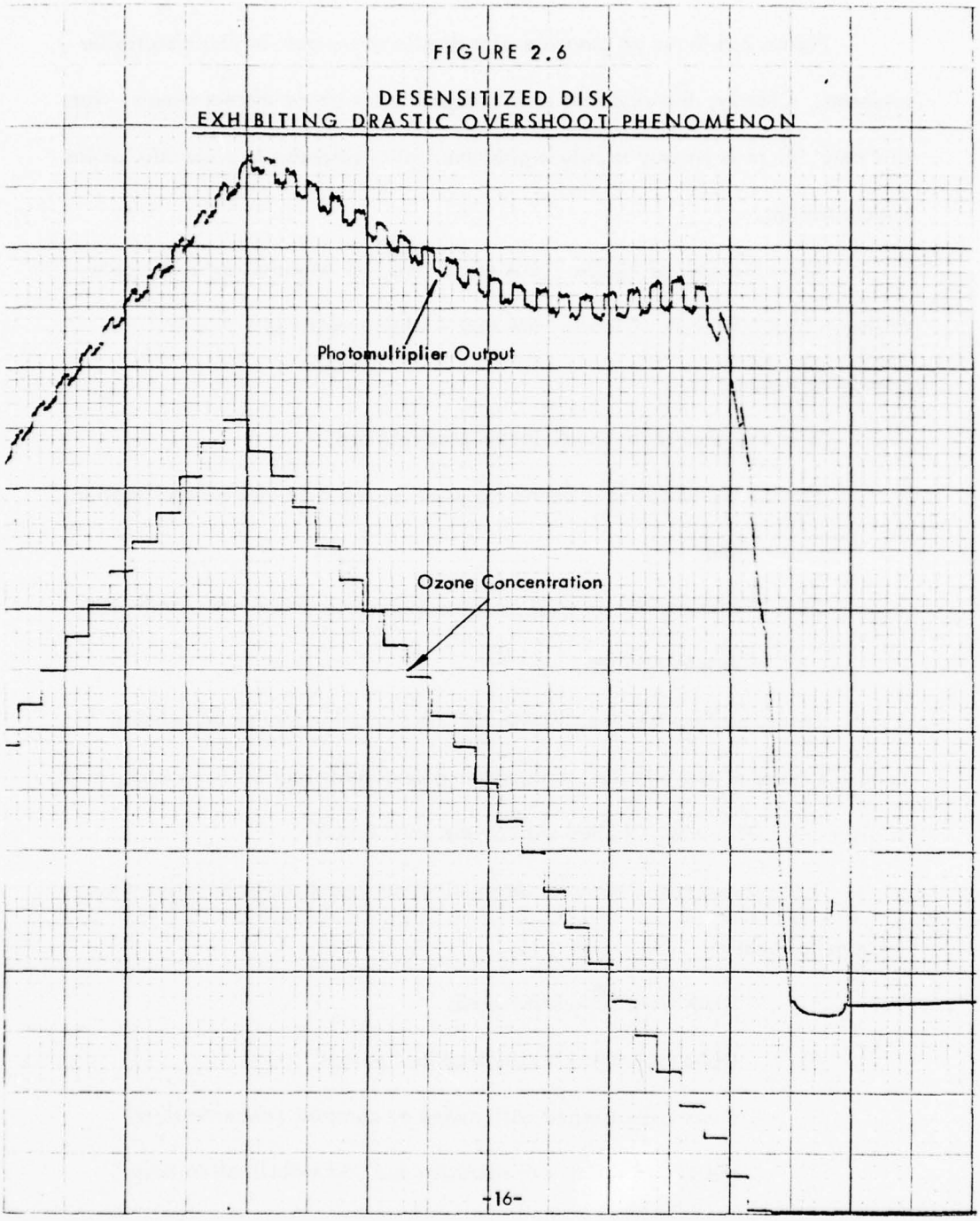

FIGURE 2.7

SENSITIZED DISK
EXHIBITING NO OVERSHOOT PHENOMENON

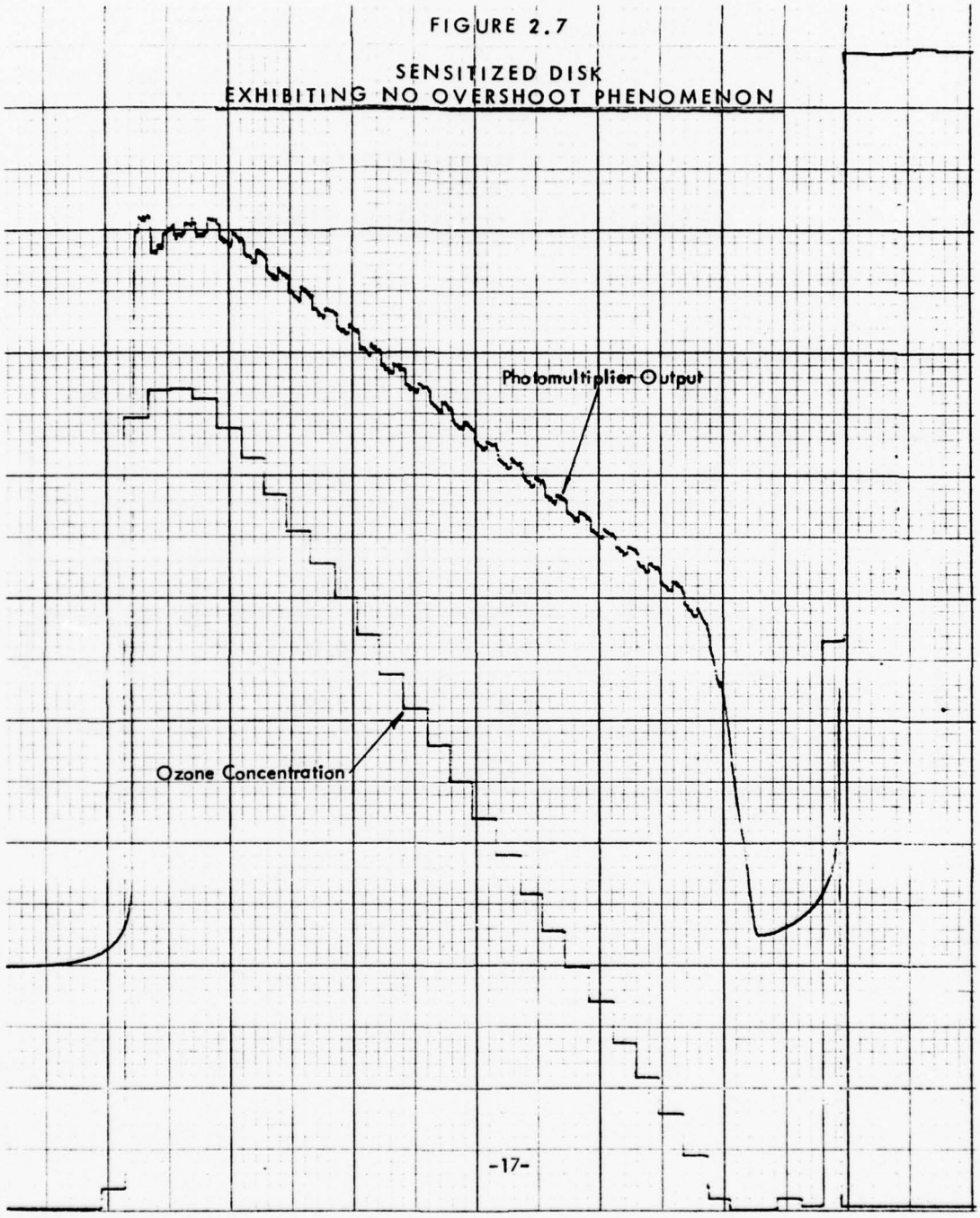

TABLE 2.1

DISK RESENSITIZATION
VERSUS
DESENSITIZATION (IDLE) TIMES

Disk #	Idle Period	Resensitization Time	Concentration (ppmV)	Flow Rate (l/min)
1104-01Y	21	11.	0.28	1
	4	2.	0.39	1
	2	1.6	0.10	1
	2	1.2	0.20	1
	2	1.6	0.265	1
	2	1.2	0.385	1

More meaningful data will be achieved if we relate resensitization by ozone flux through the sensor duct.

From Table 2.2, a zero ozone exposure period of two minutes requires an ozone flux on the order of 10^{14} molecules/second for two minutes in order to resensitize the disk.

The questions are: what is the ozone flux at high altitudes, and how long will it take to resensitize the disk with such an ozone flux?

The calculated ozone flux expected at altitude is on the order of 10^{12} molecules/second. Such a small ozone flux would require approximately two hours to fully resensitize the disk. Such a long resensitization time seemingly should preclude testing but it does not for the following reasons:

As ozone flux decreases, the magnitude of the overshoot decreases. At the low limit, despite the overshoot, the photomultiplier output is very nearly equal to the output of a stabilized disk for the same concentration, i.e., the overshoot is negligible, and it will remain negligible until greater ozone number density measurements need to be made; however, when the ozone concentration is high enough to cause the overshoot to be non-negligible, the resensitization times for those higher concentrations are shorter, on the order of two minutes. Since the descent phase of the flight is on the order of 30 - 40 minutes, a two minute resensitization time is acceptable.

Also, the ozone flux does not remain at the low level for very long. It continually increases with the increasing ozone levels present at lower altitudes.

TABLE 2.2

RESENSITIZATION TIME
VERSUS
OZONE FLUX

Disk #	Idle Period (min)	Ozone Flux (molecules/sec)	Resensitization Time (min)
1104-01Y	21	1.25×10^{14}	11
	4	1.72×10^{14}	2
	2	0.447×10^{14}	1.6
	2	0.895×10^{14}	1.2
	2	1.19×10^{14}	1.6
	2	1.72×10^{14}	1.2

Observations

The sensitivity tests led to the following observations:

1) Exposure to ozone sensitizes disks.

2) Zero ozone exposure desensitizes disks.

3) Even zero ozone exposure periods as brief as two minutes result in measurable disk desensitization.

4) The effect of disk desensitization is an overshoot in photomultiplier output, i.e., there is a greater photomultiplier response for a desensitized disk than for a sensitized one. The overshoot decreases with decreasing concentration.

5) Disks desensitized for two minutes require an ozone flux of 10^{14} molecules/second for two minutes in order to resensitize the disks.

6) During flight there will be a period of zero ozone exposure of approximately two minutes (the time between liftoff and sonde exposure to atmosphere); therefore, to resensitize disks in flight, an ozone flux of 10^{14} molecules/second for two minutes is required.

7) There is not enough ozone above 70 km altitude to accommodate the ozone flux required to resensitize flight disks; but, because the overshoot in photomultiplier output caused by desensitized disks decreases with decreasing ozone concentration,

the overshoot is low for low ozone concentrations. Above 70 km, the ozone concentration is so low that the effect of overshoot is negligible.

Conclusions

1) Disk sensitivity is compatible with rocketborne ozonesondes utilizing the chemiluminescent technique for measuring atmospheric ozone.

2) Disks must be sensitized prior to flight by flushing with 1.0 ppm ozonized air, preferably until liftoff.

3) Disks should be calibrated as close to liftoff as practical.

3.0 DETECTOR OUTPUT VERSUS CONCENTRATION

3.1 Flow Rate Dependency

Flow rates through the ozonesonde sampling duct during an actual flight are expected to vary between 6 and 300 liters per minute. Flow rates of 6 liters per minute can be readily achieved in the laboratory. Flow rates on the order of 300 liters per minute require expensive vacuum chamber/pump systems that were not available within the financial constraints of this contract; therefore, tests measuring detector output versus concentration as a function of the full range of flow rates expected during flight were not conducted. Flow rate dependency of limited scope is included in Section 3.2.

3.2 Pressure Dependency

Low pressure tests were conducted using the test setup schematicized in Figure 3.1. Essentially what was done was to sensitize the disk by flushing with ozonized air for approximately twenty minutes, then calibrating at ambient pressure, evacuating the belljar to a low pressure, resensitizing the disk, and finally calibrating at the low pressure.

Figure 3.2 compares results at ambient pressure with those at low pressure.

While the system was set up at low pressure, tests were conducted to show the effect of small changes in flow rate on detector output at low pressure. Those results are also depicted in Figure 3.2.

As shown by Figure 3.2, small changes in flow rate result in measurable detector output differences. During flight, large flow rate differences (on the order of 200 liters per minute) are expected.

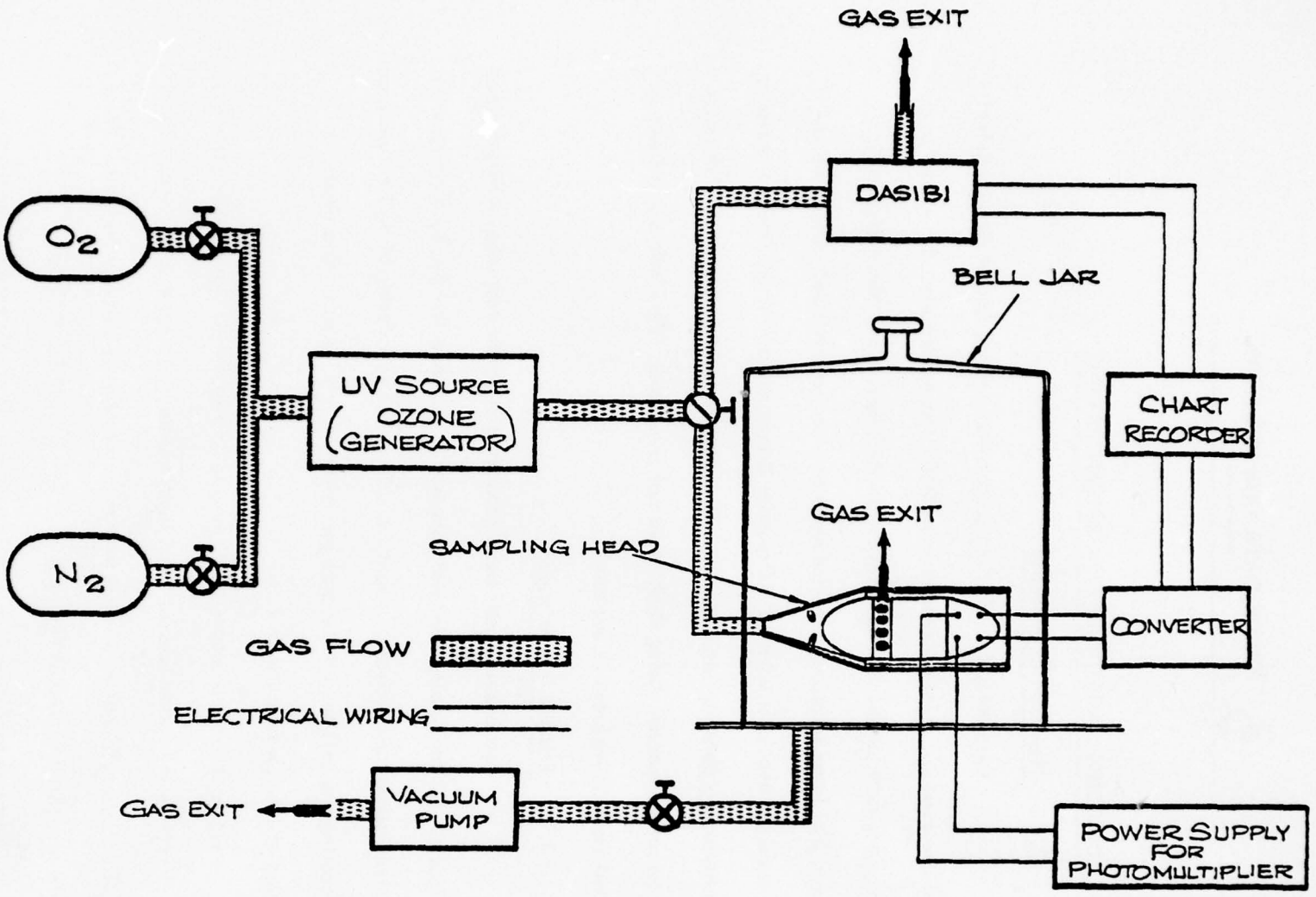

FIGURE 3.1, TEST SETUP

FIGURE 3.2
DETECTOR OUTPUT VS. CONCENTRATION,
VARYING FLOW RATE AT LOW PRESSURE

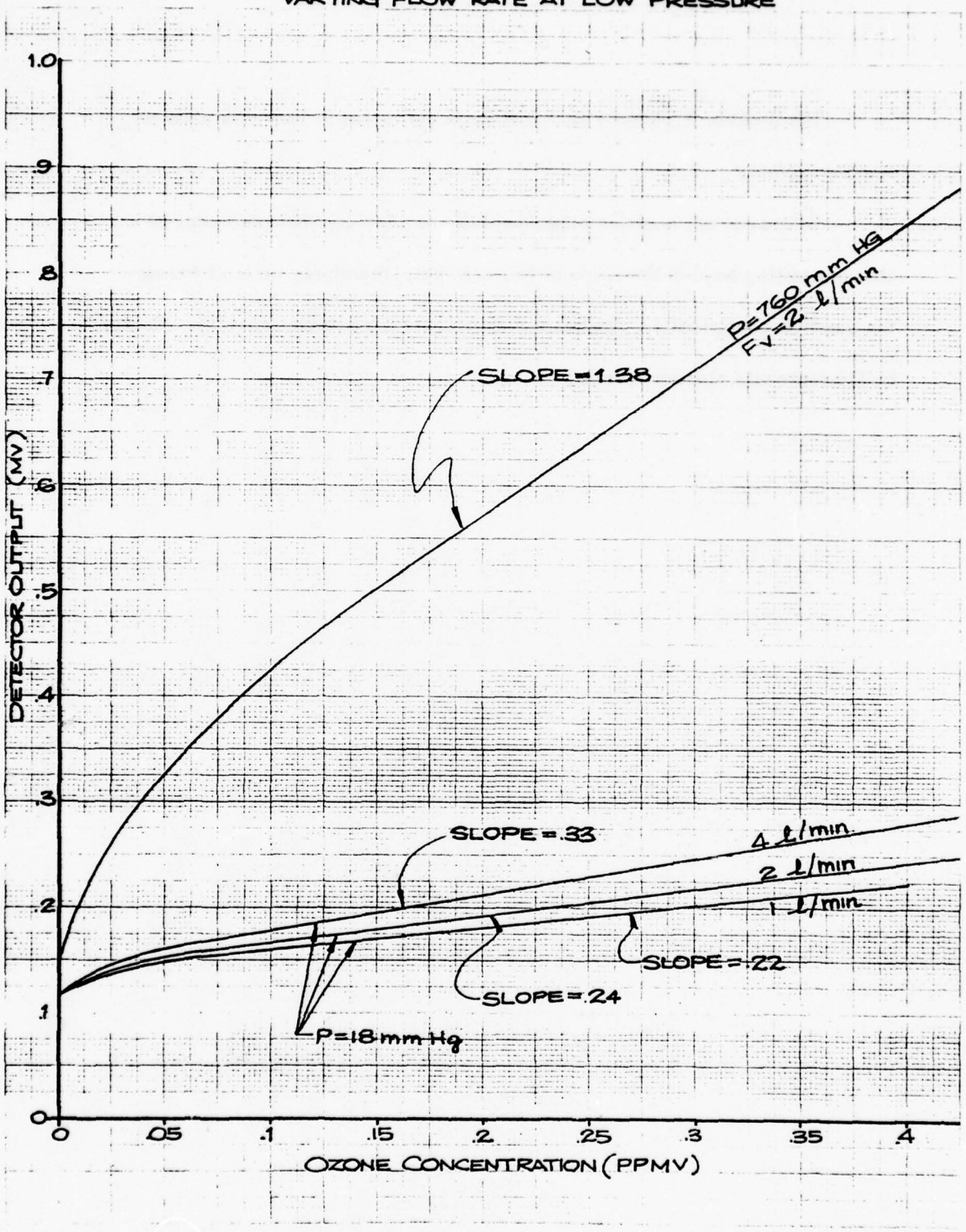

The question is, what effect will large variations in flow rate have on detector output?

To answer this question experimentally requires sophisticated vacuum chamber testing beyond the scope of this contract; therefore, we must answer the question analytically. Appendix A shows how the detector output is affected by flow rate and altitude effects.

4.0 BLOWDOWN TESTS

Previous sections have shown that atmospheric ozone data reduction depends on flow rate through the ozonesonde duct. Because in-flight flow-metering is too expensive, flow rate versus altitude is determined by calculation. The difference between the theoretical, calculated flow rate and that observed experimentally is due to friction, assuming the calculation to be otherwise correct. As a result of the blowdown test, the calculated friction factor can be adjusted to make the calculated flow rate agree with that measured in the lab. Friction factors are independent of altitude; therefore, if the flow rate calculation technique is correct, then if the calculated flow rate agrees with the observed flow rate at any one altitude (the test altitude, for example), then the calculated flow rate will agree with the observed flow rate at any and all other altitudes.

Flow rates through two ozonesonde sampling heads of different designs were measured by doing blowdown tests. Each head was mounted (in turn) into a vacuum chamber such that the ozonesonde duct entrance was at ambient pressure, and the exit was at vacuum chamber pressure. After plugging the ozonesonde duct entrance and sealing all sources of possible leaks, the vacuum chamber was evacuated to a pressure of about 60 mm of mercury. At time zero the duct entrance plug was removed; therefore, air flowed through the sampling duct into the vacuum chamber. By timing the measured pressure increase within the chamber, the flow rate through the duct was calculated, as follows:

$$F_V = \frac{V}{P}\frac{dP}{dt}$$

where F_V = volumetric flow rate

V = vacuum chamber volume

P = vacuum chamber pressure

$\frac{dP}{dt}$ = slope of chamber pressure versus time curve

This expression is derived in Appendix B.

Ozonesonde blowdown test results are plotted in Figures 4.1 and 4.2. Vacuum chamber pressure versus time is shown in Figure 4.1, while Figure 4.2 shows ozonesonde sampling duct #1 flow rate versus back pressure ratio. Back pressure ratio is the ratio of duct back pressure to duct entrance pressure.

Using techniques defined in Appendix C, the flow rate was calculated. Differences between the calculated and measured flow rates for ozonesonde design #1 are shown in Figure 4.2. To accurize flow rate calculations so that the flow rate agreed with the measured rate, loss factors were adjusted. For ozonesonde head design #1, the loss factor was changed from 6.15 to 3.90. For ozonesonde design #2, the loss factor was estimated to be 3.00.

FIGURE 4.1
OZONESONDE BLOWDOWN TEST RESULTS
VACUUM CHAMBER PRESSURE VS TIME

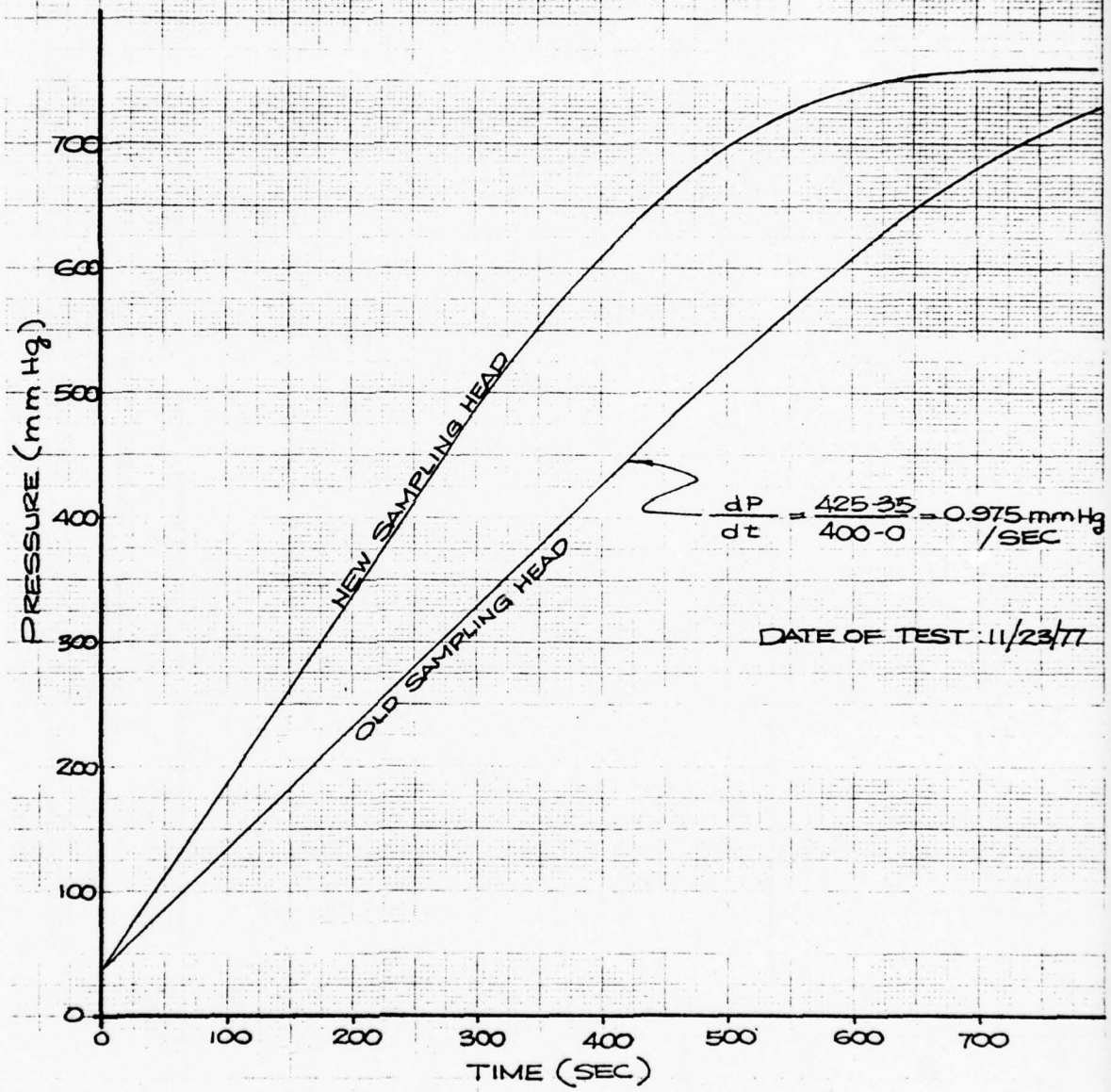

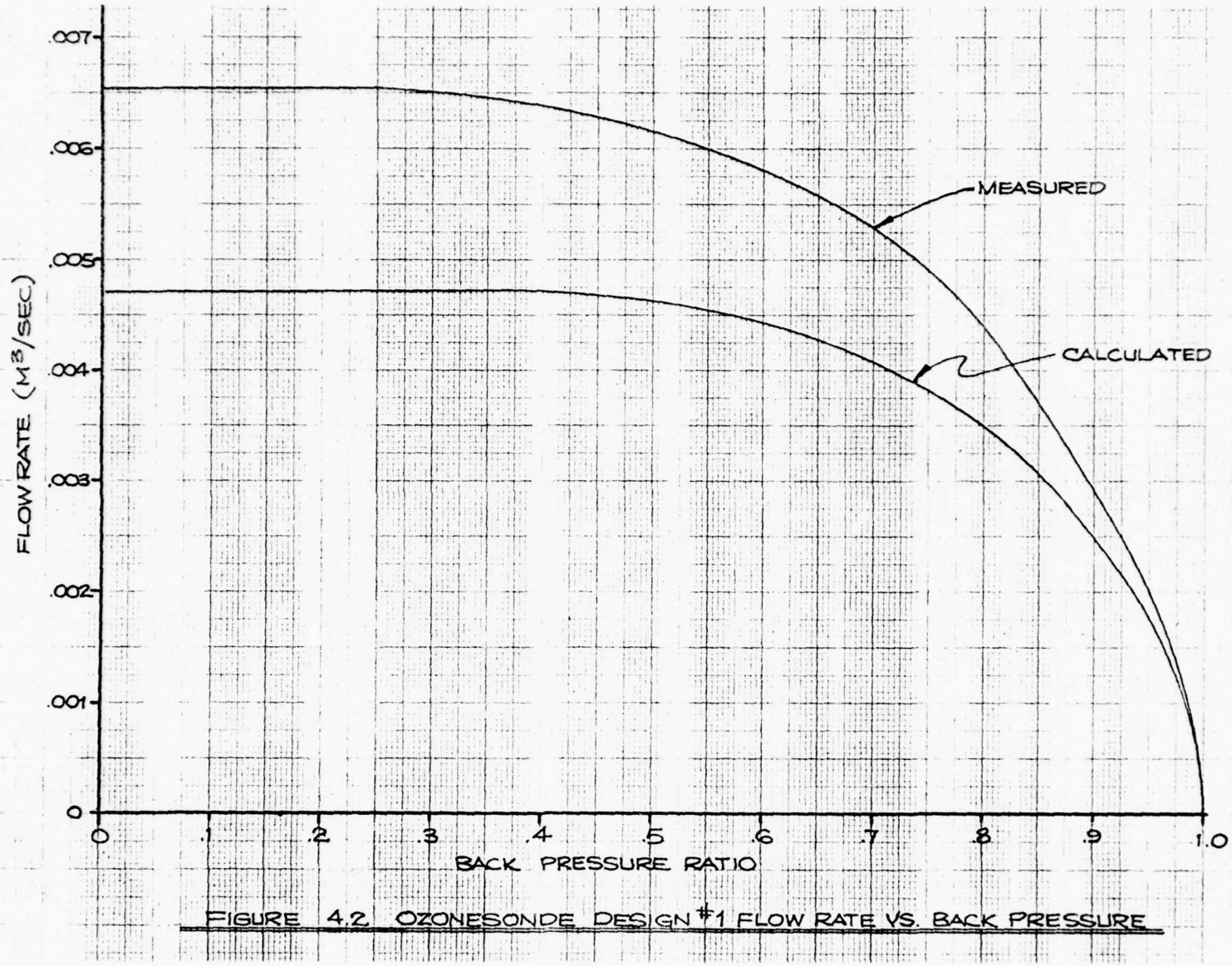

FIGURE 4.2 OZONESONDE DESIGN #1 FLOW RATE VS. BACK PRESSURE

5.0 INLET LOSSES DETERMINATION

Inlet losses were determined by first calibrating using the setup schematicized in Figure 5.1, then calibrating per the setup shown in Figure 5.2. Comparison of results yielded the inlet losses.

Within the range of tests conducted (flow rates varied from 1 to 12 liters per minute, pressures varied from 10 to 100 millibars) no significant losses were measured.

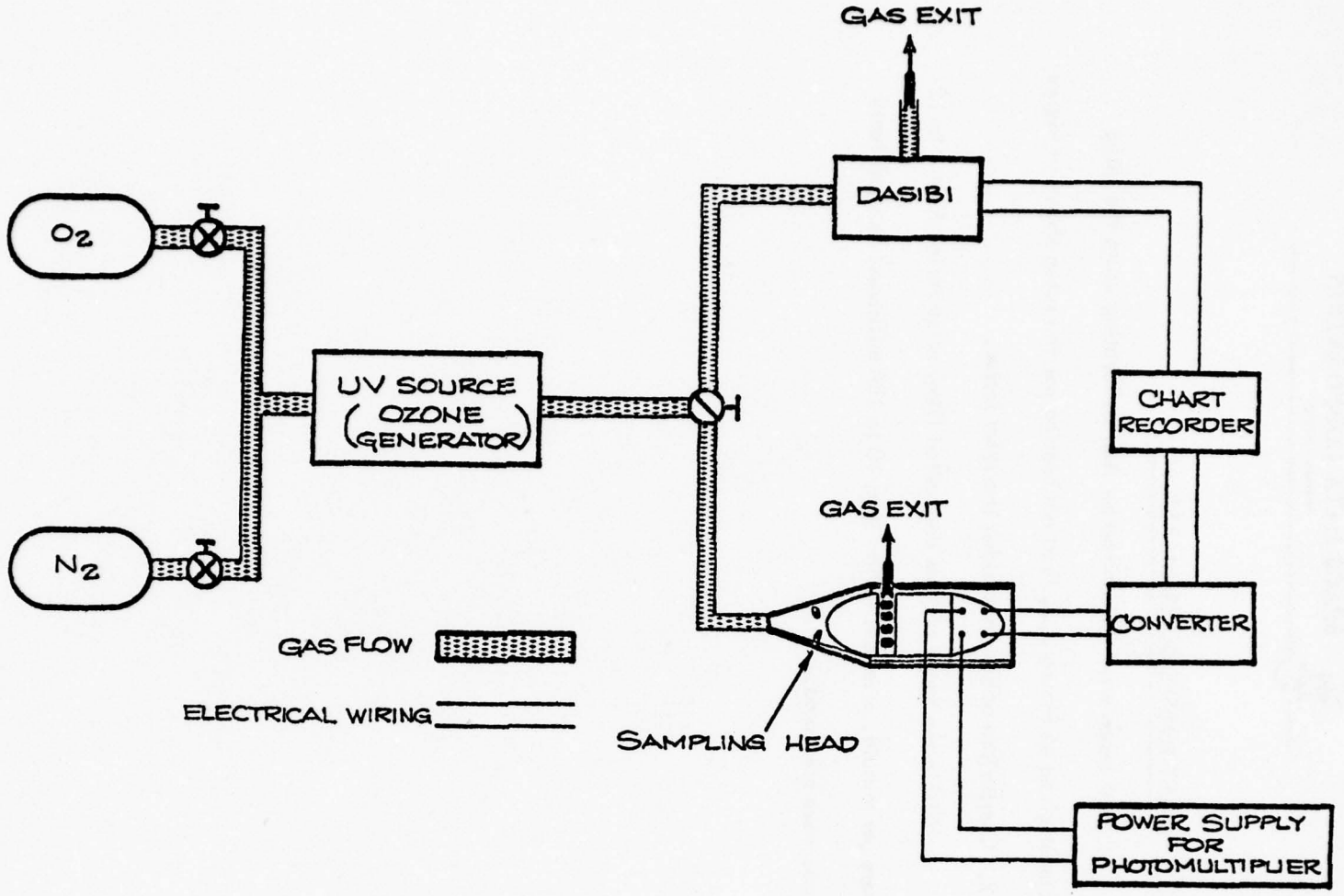

FIGURE 5.1, TEST SETUP

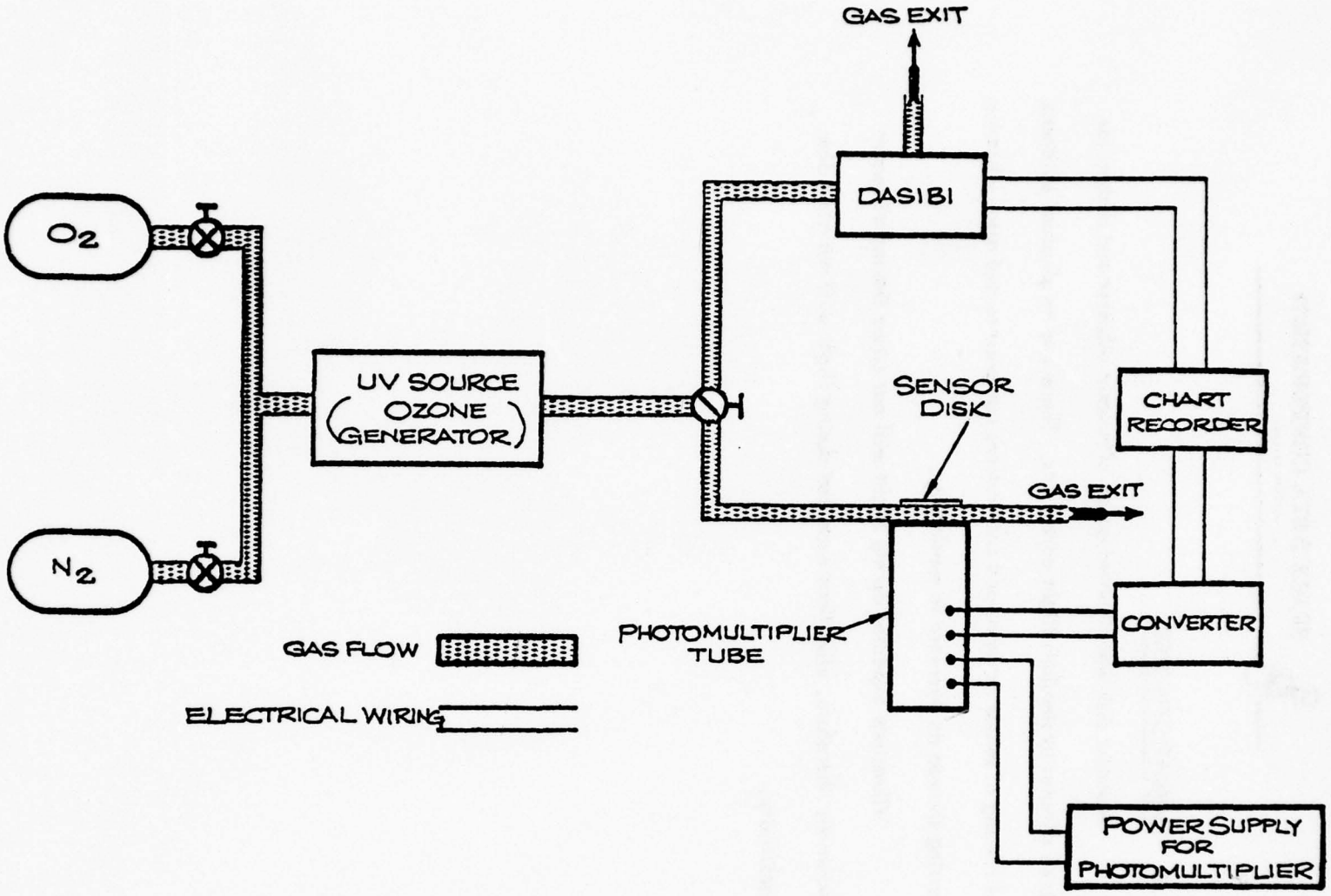

FIGURE 5.2, TEST SETUP

6.0 VIBRATIONS TEST

A sensor disk was mounted on an ultrasonic vibrator and shaken for three minutes to simulate flight conditions. There was no physical evidence of flaking of sensor material and calibrations run prior to and after vibration testing showed no decrease in sensitivity.

Vibrations expected during flight will not cause flaking of sensor material; therefore, vibrations expected during flight will not alter disk sensitivity.

7.0 THE ATMOSPHERIC OZONE DATA REDUCTION TECHNIQUE

Calibration of the detection system will be in the form of ozone concentration (ppmV) versus detector output. The calibration curve will be converted via computer to ozone number density versus detector output, as follows:

$$(N_o)_{cal} = \frac{C A_o \rho_o}{m_w} \frac{P_{cal}}{P_o} S (10)^{-6},$$

where

$(N_o)_{cal}$ = calibration ozone number density, molecules/cm^3

C = ozone concentration, ppmV

A_o = Avogadro's Number, molecules/mole

ρ_o = ozone density at reference pressure, grams/liter

m_w = ozone molecular weight, grams/mole

P_o = ozone density reference pressure, inches Hg

P_{cal} = calibration ambient pressure, inches Hg

S = conversion factor, liters/cm^3

10^{-6} = one part per million

Because

A_o = 6.02×10^{23},

ρ_o = 2.144,

P_o = 29.92,

m_w = 48, and

S = 10^{-3},

the above expression reduces to:

$$(N_o)_{cal} = 8.9871\ (10^{11})\ C\ P_{cal} \text{ molecules/cm}^3$$

Thus, the calibration curve will have been converted to ozone number density versus detector output.

Flight data acquires detector output versus altitude, which derives from the calibration curve the uncorrected ozone number density versus altitude.

Appendix A shows how the number density is corrected for flow rate and altitude effects by the factor $\frac{F_v}{\lambda}$, where F_v = volumetric flow rate, and λ = mean free path. Thus, the final data reduction expression is

$$(N_o)_{alt} = (N_o)_{cal} \times \frac{\left(\frac{F_v}{\lambda}\right)_{alt}}{\left(\frac{F_v}{\lambda}\right)_{cal}}$$, where

$(N_o)_{alt}$ = ozone number density at altitude

$(N_o)_{cal}$ = calibration number density producing the same detector output observed at altitude

$\left(\frac{F_v}{\lambda}\right)_{alt}$ = volumetric flow rate to mean free path ratio at altitude

$\left(\frac{F_v}{\lambda}\right)_{cal}$ = ratio during calibration

By reducing the data in this manner for a number of altitudes, an atmospheric ozone profile may be generated and plotted. The ozone profile shown in Figure 7.1 was generated using the data reduction technique defined in this section. The computer output for the data reduction is presented in Appendix D.

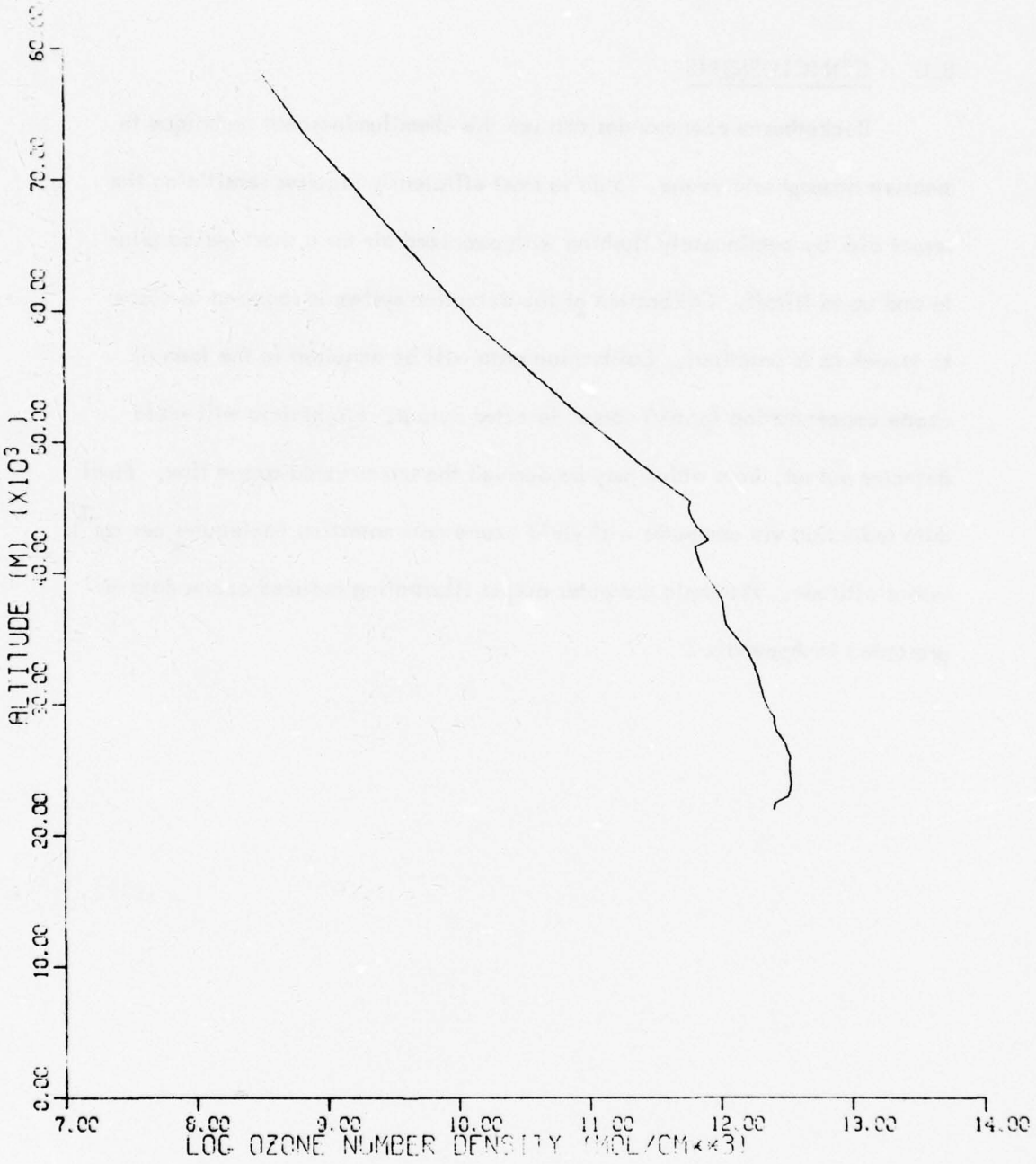

FIGURE 7.1, ATMOSPHERIC OZONE PROFILE

8.0 CONCLUSIONS

Rocketborne ozonesondes can use the chemiluminescent technique to measure atmospheric ozone. To do so most efficiently requires sensitizing the sensor disk by continuously flushing with ozonized air for a short period prior to and up to liftoff. Calibration of the detection system is required as close to launch as is practical. Calibration data will be acquired in the form of ozone concentration (ppmV) versus detector output. Flight data will yield detector output, from which may be derived the uncorrected ozone flux. Final data reduction via computer will yield ozone concentration (molecules per cm^3) versus altitude. A sample computer output illustrating reduced ozone data is presented in Appendix D.

REFERENCES

1. Pettersen, Sverre, Introduction to Meteorology, McGraw-Hill Book Company, New York, 1969.

2. Gregg, Donald C., Principles of Chemistry, Allyn and Bacon, Inc., Boston, 1963.

3. Hoffert, Martin I. and Stewart, Richard W., "Stratospheric Ozone - Fragile Shield?", Astronautics and Aeronautics, October, 1975.

4. Stegman, D. H., "Measurement Techniques for the Ozone Layer," Research/Development, January, 1976.

5. Boruki, W. J., et. al., "Model Predictions of Latitude-Dependent Ozone Depletion Due to Supersonic Transport Operations," AIAA Journal, December, 1976.

APPENDIX A

THE DATA REDUCTION EQUATION

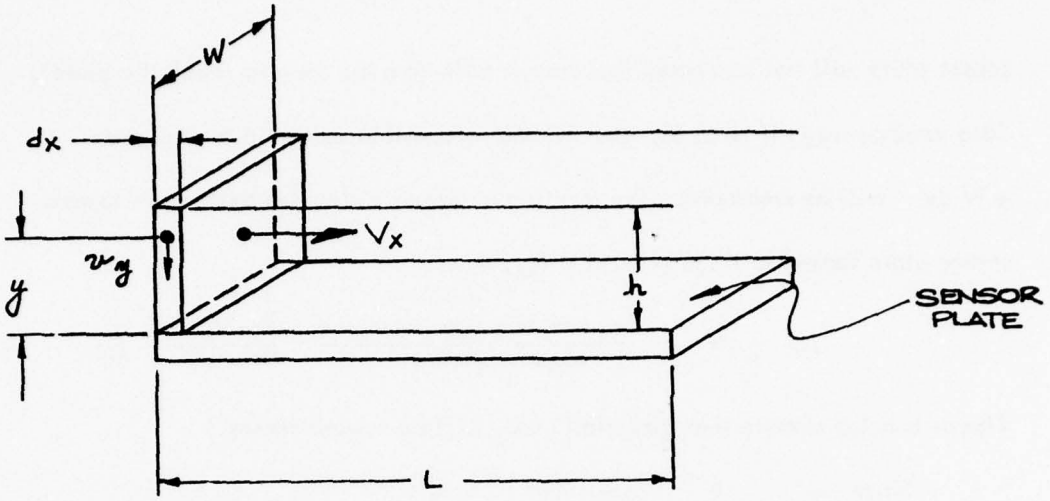

If an ozone molecule is a distance y from the sensor plate, then the time it takes the molecule to diffuse to the plate is:

$$\frac{y}{t_y} = V_y \Longrightarrow t_y = \frac{y}{V_y}$$

where V_y = diffusion velocity

If t_x is the time in which the elemental volume moves down the tube,

then $t_x = \frac{x}{V_x}$, where $V_x = \frac{F_V}{A}$

where F_V = flow rate

A = cross-sectional area of duct

($A = hW$)

Then:

$t_c = \frac{L}{V_x} = \frac{LA}{F_V}$ = critical time. This is the time that the elemental volume is in contact with the sensor plate.

Now then, if $t_y > t_c$, then the ozone molecule a distance y from the

sensor plate will not be sensed (because it will take too long to reach the plate). Said another way, if $t_y \leq t_c$, then all the measurable ozone in the volume $y\,W\,dx$ will be measured. The fraction of ozone molecules that moves toward sensor plate sensed to those present is f_M, where

$$f_M = \frac{\text{volume of ozone measured}}{\text{volume present}} = \frac{\frac{1}{6}\, y\, W\, dx}{h\, W\, dx} = \frac{y}{6h}$$

(There is a 1:6 chance that direction of V_y will be toward sensor.)

Since y = such that $t_y \leq t_c$

$$\Longrightarrow \frac{y}{V_y} \leq \frac{LA}{F_V} \Longrightarrow y \leq \frac{LAV_y}{F_V}$$

Since $A = hW$, $y \leq LhW \frac{V_y}{F_V}$

Thus $f_M = \frac{y}{6h} = \frac{LhW}{6h} \frac{V_y}{F_V} = \frac{LW\,V_y}{6\,F_V}$

i.e., the fraction of ozone measured to ozone present is:

$$f_M = \frac{LW\,V_y}{6\,F_V}$$

where f_M = the fraction

L = sensor length

W = sensor width

V_y = diffusion velocity

F_V = flow rate

What does all this mean?

When we measure ozone, we get a reading θ which indicates how much ozone is measured. This is not necessarily the amount of ozone present. In fact,

$$\text{amount of ozone present} = \frac{\text{amount of ozone measured}}{F_M}$$

$$\text{i.e., } F_M = \frac{\text{(ozone) measured}}{\text{(ozone) present}} \Longrightarrow \text{(ozone) present} = \frac{\text{(ozone) measured}}{f_M}$$

$$\text{Since } F_M = \frac{L\,W}{6}\,\frac{V_y}{F_V}$$

$$\text{(ozone present)} = \frac{6\,[\,\text{(ozone) measured}]\,F_V}{LW\,V_y}$$

This is, essentially, the data reduction equation.

What we must do now is relate a calibration to altitude measurements.

During calibration we have:

$$(Oz)\text{ present} = 6 \times (Oz)\text{ measured} \times \frac{F_V}{LW\,V_y}$$

$$V_y = k\lambda\,,$$

where λ = mean free path

k = constant.

This says that the diffusion velocity is proportional to the mean free path; the greater the mean free path, the fewer the collisions and the faster the diffusion rate.

Thus, during calibration we have:

$$(Oz)_{present} = 6 \times \frac{(Oz)_{measured} \times F_V}{LW\,V_y} = 6 \times \frac{(Oz)_{measured} \times F_V}{LWk\lambda}$$

and we can plot: θ versus (Oz) measured, as follows:

Calibration

θ	$(Oz)_{measured}$
θ_1	$(No)_1$
θ_2	$(N_o)_2$
θ_3	$(N_o)_3$
.	.
.	.
.	.
θ_n	$(N_o)_n$

And we know: $(Oz)_{present}$, F_V, L, W, and λ .

During flight we measure θ, and we have:

θ	$(Oz)_{measured}$
θ_{1F}	$(N_o)_{1F}$
θ_{2F}	$(N_o)_{2F}$
θ_{3F}	$(N_o)_{3F}$
.	.
.	.
.	.
θ_{nF}	$(N_o)_{nF}$

Then: $[(Oz)_{present}]_{flight} = 6x\,[(oz)_{measured}]_{flight} \dfrac{(F_V)_{flight}}{LWk\,\lambda\,flight}$

We can now relate flight data to calibration, as follows:

$$\frac{[(Oz)_{present}]_{flight}}{[(Oz)_{present}]_{cal}} = \frac{\frac{6\ F_V)_{flight}}{LWk\ \lambda\ flight}}{\frac{6\ (F_V)}{LWk\ \lambda\ cal}} \times \frac{[(Oz)_{measured}]_{flight}}{[(Oz)_{measured}]_{cal}}$$

We will now let $[(Oz)_{measured}]_{flight} = [(Oz)_{measured}]_{cal}$, i.e., $\theta_{flight} = \theta_{cal}$.

L, W, and k are constant, and not functions of altitude.

Equation reduces to:

$$\frac{[(Oz)_{present}]_{flight}}{[(Oz)_{present}]_{cal}} = \frac{(F_V)_{flight}\ \lambda_{cal}}{\lambda\ flight\ (F_V)_{cal}}$$

or

$$[(Oz)_{present}]_{flight} = [(Oz)_{present}]_{cal} \times \frac{(F_V)_{flight}}{(F_V)_{cal}} \times \frac{\lambda\ cal}{\lambda\ flight}$$

This is the data reduction equation.

Thus, the data reduction equation:

$$[(Oz)_{present}]_{flight} = [(Oz)_{present}]_{cal} \times \frac{(F_V)_{flight}}{(F_V)_{cal}} \times \frac{\lambda\ cal}{\lambda\ flight}$$

where

$[(Oz)_{present}]_{cal}$ = number density of ozone in lab that produced the same θ reading as we get at altitude

$(F_V)_{flight}$ = volumetric flow rate at altitude, calculated by computer from pressures, density, fall velocity, etc.

λ flight = mean free path at altitude (tabulated in standard atmosphere, 1976)

$(F_V)_{cal}$ = calibration flow rate

λ_{cal} = mean free path at calibration altitude

APPENDIX B
BLOWDOWN TEST FLOW RATE DERIVATION

Volumetric flow rate will be determined using the vacuum chamber pressure versus time curve, the known (constant) volume of the vacuum chamber, and the assumptions that the air acts as an ideal gas and the temperature remains constant.

Thus, the equation of state for an ideal gas can be used:

$$P_2 = \rho RT,$$

where

P_2 = Vacuum chamber pressure

ρ = Density of air in chamber

R = Universal gas constant

By definition, $\rho = \frac{m}{V}$, where m = mass of air in vacuum chamber, V = chamber volume

Thus, $d\rho = \frac{1}{V} dm$ (V is constant)

Since $P_2 = \rho RT$,

$dP_2 = RT\, d\rho$ (R is constant, T is assumed constant)

or,

$$dP_2 = \frac{RT}{V} dm$$

$$\frac{dm}{dt} = \frac{V}{RT} \frac{dP_2}{dt} = \text{mass flow rate entering chamber} = \rho F_v,$$

where F_v = volumetric flow rate

Thus, $$\rho F_v = \frac{V}{RT} \frac{dP_2}{dt}$$

$$F_v = \frac{V}{\rho RT} \frac{d P_2}{dt}$$

Since $P_2 = \rho RT$ from equation of state,

$$F_v = \frac{V}{P_2} \frac{dP_2}{dt}$$

APPENDIX C

OZONESONDE DUCT FLOW RATE CALCULATION

The following is an excerpt from SDC TM-1414, "Ozonesonde Duct Flow Rate Calculation."

2.7 Final Flow Rate Equation

The results of Sections 2.1 through 2.7 are conglomerated to achieve the technique for calculating the flow rate through the ozonesonde sampling duct at a given altitude. The solution is as follows:

In general,

$$F_V = \frac{A\beta\sqrt{\frac{P_\infty}{\rho_\infty}\left(1-\frac{P_V}{P_T}\right)}}{\sqrt{\alpha L_F + L_M + 0.5\left(\frac{A}{A_{exit}}\right)^2}} + K_F\left(\frac{1+2.507\,d/2\lambda}{1+3.095\,d/2\lambda}\right)\left(1-\frac{P_V}{P_T}\right)$$

Before the final solution can be achieved, we must evaluate the compressibility (β), determine whether flow is laminar or turbulent (and thereby establish α), and we must determine whether the flow is in the continuum or transition flow regime.

The solution thus is achieved by trial and error and is best achieved via computer.

The quantities A, A_{exit}, L_F, L_M, d, and K_F are functions of the duct configuration and are constant throughout the flight.

The quantities P_∞, ρ_∞, and λ are functions of the altitude in question.

P_V and P_T are calculated as functions of P_∞ and sonde fall velocity, U_∞ as given in Section 2.1.

α and β are functions of the flow rate. Therefore, their values must be assumed to achieve the first approximation. The first approximation will give us an idea of whether the flow is laminar or turbulent and of what the compressibility may be.

The solution technique is outlined as follows:

1) Using the methods of Section 2.1, calculate $\frac{P_V}{P_T}$

2) Evaulate β, as follows:

If $\frac{P_V}{P_T} > .84$, $\beta = 1.$

If $\frac{P_V}{P_T} < .63$, $\beta = 0.7936.$

If $.63 \leq \frac{P_V}{P_T} \leq .84$, $\beta = 4.2404\left(\frac{P_V}{P_T} - .63\right)^2 + 0.7936$

3) Let $\alpha = 1.$

4) Determine P_∞ and ρ_∞ for the altitude in question.

5) Calculate

$$\frac{A\beta\sqrt{\frac{P_\infty}{\rho_\infty}\left(1-\frac{P_V}{P_T}\right)}}{\sqrt{\alpha L_F + L_M + 0.5\left(\frac{A}{A_{exit}}\right)^2}} = F_i$$

6) Calculate M_1, the flow mach number at entrance

$$\frac{F_i}{0.91\, a_\infty A_{in}},$$

where F_i is the quantity evaluated in Step 5),

a_∞ = speed of sound at altitude in question,

A_{in} = duct entrance area

7) If $M_1 < 1$ and if $\beta = 1$, calculate Reynolds number per Step 8).

If $M_1 < 1$ and $\beta \neq 1$, then change β to 1 and recalculate F_i.

8) If $M_1 \geq 1$ (or if $M_1 < 1$ and $\beta = 1$),

$$R_e = \frac{F_i}{A} \frac{\rho_\infty d}{\mu_\infty} = \text{Reynolds Number}$$

9) If $R_e \geq 800$, flow is turbulent and assumption that $\alpha = 1$ was valid

If $R_e < 800$, $\alpha = \frac{800}{R_e}$, and you must recalculate F_i.

(i.e., return to Step 5) and redo 5) through 8)

10) R_e' = new Reynolds Number. If R_e' is within 10% of the old Reynolds number, α approximation is close.

11) Calculate the ratio $d/2\lambda$, the ratio used to determine the flow regime.

12) If $d/2\lambda = \geq 100$, continuum flow exists, and $F_V = F_i$.

13) If $d/2\lambda = \leq 0.1$, purely free molecular flow exists, and $F_V = K_F \left(1 - \frac{P_V}{P_T}\right)$.

14) If $0.1 < \frac{d}{2\lambda} < 100$, transitional flow exists, and

$$F_V = F_i + Z K_F \left(1 - \frac{P_V}{P_T}\right), \text{ where}$$

$$Z = \frac{1 + 2.507\, d/2\lambda}{1 + 3.095\, d/2\lambda}$$

F_V = flow rate at the altitude in question

A = duct cross-sectional area (in sensing chamber)

A_{exit} = duct exit area

A_{in} = duct entrance area

d = duct hydraulic radius (in sensing chamber)

L_F = friction factor

L_M = momentum loss factor

K_F = duct conductance

P_∞ = ambient pressure at altitude

ρ_∞ = ambient air density at altitude

μ_∞ = viscosity of air at altitude

λ = mean free path at altitude

a_∞ = speed of sound at altitude

U_∞ = sonde fall velocity at altitude

P_V = Venturi pressure

P_T = total pressure incident to duct = $P_\infty + \frac{1}{2} \rho_\infty U_\infty^2$

α = friction parameter

β = compressibility parameter

2.1 Calculation of P_V, the Venturi Pressure

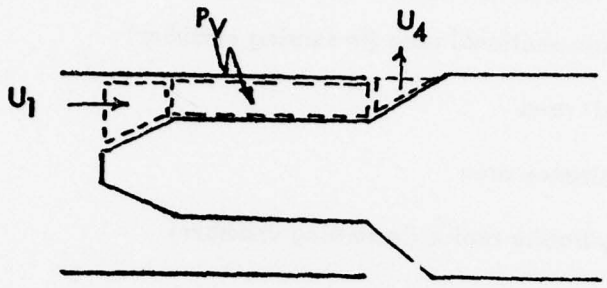

Assume isentropic flow (no losses). Flow characteristics can be determined using isentropic flow tables.

$ARAT1 = \frac{A_4}{A^*}$. If $A^* > A_{throat}$, then M = 1 in throat.

Thus, for all ARAT1 such that $\frac{A_4}{A^*} < \frac{A_4}{A_{throat}}$, M = 1 at throat.

($A^* > A_{throat} \Rightarrow \frac{A_4}{A^*} < \frac{A_4}{A_{throat}}$.)

From the Appendix, $A_{throat} = .2167\ in^2$ and $A_4 = .7854\ in^2$. Thus,

$$A_{throat} = A_2 = 0.2167\ in^2, \quad \frac{A_4}{A_2} = \frac{0.7854}{0.2167} = 3.6244$$

$\therefore$ For all ARAT1, such that $\frac{A_4}{A^*} < 3.6244$, M = 1 at throat.

This corresponds to $\frac{P_4}{P_t}$ of $< .982$. Thus, for all $\frac{P_4}{P_t} < .982$,

$P_V = 0.5283\ P_T$. Since $P4 = P_\infty$, M = 1 at throat for $\frac{P_\infty}{P_T} < .982$.

For $\frac{P_4}{P_t} \geq .982$, $\frac{A_4}{A^*} \geq 3.6244$, subsonic flow exists in throat, and P_V is found using isentropic flow tables.

Summary of calculation of P_V using isentropic flow tables:

1) Calculate PRAT11 = $\frac{P_\infty}{P_T}$ If PRAT11 < .982,

$P_V = .5283\ P_T$.

2) Look up PRAT11 in isentropic flow tables. Find corresponding ARAT11 ($ARAT11 = A_4/A^*$).

3) Calculate ARAT22, where ARAT11 = ARAT11/3.6244.

4) Look up ARAT22 in isentropic flow tables (subsonic section). Find corresponding PRAT22.

5) PRAT22 = $\frac{P_V}{P_T}$. So $P_V = PRAT22 * P_T$.

APPENDIX D
SAMPLE OZONE PROFILE REDUCED DATA

OZONESONDE CONFIGURATION PARAMETERS

VENTURI THROAT AREA	=	0.2167 IN**2
VENTURI EXIT AREA	=	0.7854 IN**2
SAMPLING DUCT ENTRANCE AREA	=	0.50320E-04 M**2
SAMPLING DUCT EXIT AREA	=	0.67097E-04 M**2
SENSING CHAMBER CROSS-SECTIONAL AREA	=	0.80645E-04 M**2
SENSING CHAMBER HYDRAULIC RADIUS	=	0.56388E-02 METERS
FRICTION LOSS PARAMETER	=	1.5620 (DIMENSIONLESS)
MOMENTUM LOSS PARAMETER	=	4.5870 (DIMENSIONLESS)
DUCT CONDUCTANCE	=	0.00417 M**3/SEC

CALIBRATION PARAMETERS

CALIBRATION ALTITUDE	=	1100.00	FEET
CALIBRATION FLOW RATE	=	1.0000	LITERS / MINUTE
CALIBRATION AMBIENT PRESSURE	=	29.8900	INCHES OF MERCURY
CALIBRATION AMBIENT TEMPERATURE	=	65.0000	DEGREES FAHRENHEIT

CALIBRATION DATA

DETECTOR OUTPUT (RATIO)	CONCENTRATION (PPMV)
0.6315	0.5000
0.6164	0.4750
0.5959	0.4500
0.5744	0.4250
0.5636	0.4000
0.5474	0.3750
0.5323	0.3500
0.5086	0.3250
0.4989	0.3000
0.4806	0.2750
0.4612	0.2500
0.4440	0.2250
0.4310	0.2000
0.4127	0.1750
0.3933	0.1500
0.3642	0.1250
0.3384	0.1000
0.3039	0.0750
0.2651	0.0500
0.2155	0.0250
0.1616	0.0000

METEOROLOGICAL ROCKET DATA (OPTIONAL)

MEASURED MET ROCKET DATA IS USED BETWEEN 70000.00 AND 25000.00 METERS

ALTITUDE (METERS)	PRESSURE (MBARS)	DENSITY (G/M**3)	TEMP (DEG K)	SPEED OF SOUND (METERS/SECOND)
70000.100	0.5500E-01	0.8500E-01	226.5000	301.8300
69000.000	0.6400E-01	0.9500E-01	233.0000	306.1200
68000.000	0.7300E-01	0.1070E+00	238.1000	309.4700
67000.000	0.8400E-01	0.1210E+00	242.5000	312.2800
66000.000	0.9700E-01	0.1360E+00	246.6000	314.9300
65000.000	0.1100E+00	0.1540E+00	249.3000	316.6500
64000.000	0.1260E+00	0.1760E+00	249.9000	317.0400
63000.000	0.1440E+00	0.2010E+00	249.7000	316.9200
62000.000	0.1650E+00	0.2300E+00	249.8000	316.9900
61000.000	0.1890E+00	0.2630E+00	249.8000	316.9300
60000.000	0.2160E+00	0.3010E+00	250.1000	317.1400
59000.000	0.2470E+00	0.3390E+00	253.6000	319.3700
58000.000	0.2810E+00	0.3820E+00	256.4000	321.1300
57000.000	0.3200E+00	0.4310E+00	258.9000	322.7100
56000.000	0.3650E+00	0.4890E+00	259.8000	323.2100
55000.000	0.4150E+00	0.5590E+00	258.5000	322.4500
54000.000	0.4730E+00	0.6350E+00	259.3000	322.9500
53000.000	0.5380E+00	0.7180E+00	260.7000	323.8300
52000.000	0.6110E+00	0.8130E+00	262.0000	324.6200
51000.000	0.6950E+00	0.9200E+00	263.2000	325.3500
50000.000	0.7890E+00	0.1043E+01	263.7000	325.6400
49000.000	0.8970E+00	0.1193E+01	261.9000	324.5500
48000.000	0.1020E+01	0.1365E+01	260.4000	323.6100
47000.000	0.1161E+01	0.1542E+01	262.2000	324.7100
46000.000	0.1319E+01	0.1738E+01	264.4000	326.1000
45000.000	0.1498E+01	0.1986E+01	262.9000	325.1400
44000.000	0.1704E+01	0.2280E+01	260.4000	323.5900
43000.000	0.1941E+01	0.2622E+01	257.9000	322.0700
42000.000	0.2212E+01	0.2997E+01	257.1000	321.5600
41000.000	0.2523E+01	0.3431E+01	256.1000	320.9600

40000.000	0.2880E+01	0.3971E+01	252.7000	318.7900
39000.000	0.3294E+01	0.4604E+01	249.3000	316.6300
38000.000	0.3775E+01	0.5349E+01	245.8000	314.4400
37000.000	0.4335E+01	0.6229E+01	242.4000	312.2500
36000.000	0.4987E+01	0.7269E+01	239.0000	310.0500
35000.000	0.5750E+01	0.8499E+01	235.7000	307.8800
34000.000	0.6637E+01	0.9851E+01	234.7000	307.2600
33000.000	0.7672E+01	0.1153E+02	231.9000	305.3700
32000.000	0.8879E+01	0.1342E+02	230.5000	304.4800
31000.000	0.1028E+02	0.1550E+02	231.1000	304.8700
30000.000	0.1191E+02	0.1821E+02	227.9000	302.7400
29000.000	0.1383E+02	0.2130E+02	226.2000	301.6000
28000.000	0.1609E+02	0.2537E+02	220.9000	298.0400
27000.000	0.1876E+02	0.2970E+02	220.0000	297.4700
26000.000	0.2188E+02	0.3478E+02	219.2000	296.8900
25000.000	0.2555E+02	0.4077E+02	218.3000	296.3000

NUMBER OF ELEMENTS IN PRESSURE TABLE = 46
NUMBER OF ELEMENTS IN DENSITY TABLE = 46
NUMBER OF ELEMENTS IN TEMPERATURE TABLE = 46
NUMBER OF ELEMENTS IN SPEED OF SOUND TABLE = 46

FLIGHT TABLES

ALTITUDE (METERS)	VELOCITY (M/SEC)	TIME (SEC)
78896.00	119.0000	140.2000
78637.00	140.0000	142.2000
77707.00	175.0000	148.2000
76941.00	202.0000	152.2000
75868.00	226.0000	157.2000
74941.00	240.0000	161.2000
73961.00	246.0000	165.2000
73000.00	260.0000	169.2000
72000.00	265.0000	173.2000
71000.00	265.0000	177.2000
70000.00	260.0000	181.2000
69108.00	248.0000	184.2000
68127.00	241.0000	188.2000
67179.00	232.0000	192.2000
66051.00	219.0000	197.2000
65193.00	208.0000	201.2000
64005.00	187.0000	207.2000
63274.00	177.0000	211.2000
62092.00	161.0000	218.2000
61014.00	149.0000	225.2000
60011.00	137.0000	232.2000
59073.00	131.0000	239.2000
58066.00	120.0000	247.2000
57017.00	112.0000	256.1400
56041.00	105.0000	265.2000
55017.00	93.0000	275.2000
54062.00	91.0000	285.2000
53006.00	85.0000	297.2000
52018.00	80.0000	309.2000
51073.00	77.0000	321.0000
50038.00	70.0000	335.2000
48005.00	64.0000	365.2000
46043.00	56.0000	398.2000
44570.00	50.0000	426.2000
43801.00	47.0000	442.2000

42005.00	42.0000	483.2000
40020.00	38.0000	535.2000
38149.00	32.0000	591.2000
36090.00	25.0000	663.2000
34033.00	24.0000	747.2000
30000.00	16.0000	955.2000
26039.00	12.0000	1247.2000
24004.00	10.0000	1443.2000
22020.00	8.0000	1675.2000
20051.00	7.0000	1939.2000

NUMBER OF ELEMENTS IN VELOCITY TABLE = 45
NUMBER OF ELEMENTS IN TIME TABLE = 45

OZONE TEST DATA

1	OZONE TIME/REF/DATA =	1677.899999	92.000000	26.000000
2	OZONE TIME/REF/DATA =	1620.000000	92.000000	26.000000
3	OZONE TIME/REF/DATA =	1590.000000	92.000000	28.000000
4	OZONE TIME/REF/DATA =	1470.000000	92.000000	30.000000
5	OZONE TIME/REF/DATA =	1170.000000	92.000000	32.000000
6	OZONE TIME/REF/DATA =	1080.000000	92.000000	31.000000
7	OZONE TIME/REF/DATA =	1050.000000	92.000000	32.000000
8	OZONE TIME/REF/DATA =	600.000000	92.000000	31.500000
9	OZONE TIME/REF/DATA =	540.000000	92.000000	32.000000
10	OZONE TIME/REF/DATA =	480.000000	92.000000	30.000000
11	OZONE TIME/REF/DATA =	420.000000	92.000000	26.000000
12	OZONE TIME/REF/DATA =	360.000000	92.000000	22.000000
13	OZONE TIME/REF/DATA =	300.000000	92.000000	19.000000
14	OZONE TIME/REF/DATA =	240.000000	92.000000	16.900000
15	OZONE TIME/REF/DATA =	168.000000	92.000000	15.800000
16	OZONE TIME/REF/DATA =	0.000000	92.000000	15.800000

COMPUTATION INFORMATION

INITIAL ALTITUDE	=	78500.00	METERS
COMPUTATION INTERVAL	=	500.00	METERS
CUTOFF ALTITUDE	=	22000.00	METERS

MEASURED MET VALUES ARE USED BETWEEN 70000. AND 25000. METERS.

SUPER LOKI FLIGHT 0025 OZONESONDE S/N 104 25 MAR 77 0200 HRS WSMR

ALTITUDE (METERS)	FLOW RATE (M**3/SEC)	REYNOLDS NUMBER	83 N.D. CONC. (1/CM**3)	VELOCITY (M/SEC)	PRESSURE ATM. (KGF/M**2)	DENSITY ATM. (KGF*S**2/M**4)	TEMP ATM. (DEG K)	DYNAMIC VISCOSITY (KGF*S/M**2)
78500.00	0.1999E-02	0.3667E-01	0.2979E+09	145.1559	0.1390E+00	0.2401E-05	201.5655	0.1364E-05
78000.00	0.2003E-02	0.4056E-01	0.3260E+09	163.9731	0.1496E+00	0.2574E-05	202.5410	0.1369E-05
77500.00	0.2012E-02	0.4607E-01	0.3507E+09	182.2563	0.1640E+00	0.2805E-05	203.5173	0.1375E-05
77000.00	0.2021E-02	0.5175E-01	0.3790E+09	199.9204	0.1785E+00	0.3036E-05	204.4935	0.1381E-05
76500.00	0.2028E-02	0.5761E-01	0.4118E+09	211.8639	0.1929E+00	0.3267E-05	205.4698	0.1386E-05
76000.00	0.2035E-02	0.6362E-01	0.4503E+09	223.0475	0.2073E+00	0.3499E-05	206.4460	0.1392E-05
75500.00	0.2047E-02	0.7207E-01	0.4846E+09	231.5577	0.2269E+00	0.3807E-05	207.4228	0.1397E-05
75000.00	0.2059E-02	0.8079E-01	0.5237E+09	239.1090	0.2465E+00	0.4114E-05	208.3995	0.1403E-05
74500.00	0.2069E-02	0.8976E-01	0.5689E+09	242.7000	0.2660E+00	0.4422E-05	209.3763	0.1409E-05
74000.00	0.2079E-02	0.9897E-01	0.6219E+09	245.7612	0.2856E+00	0.4730E-05	210.3530	0.1414E-05
73500.00	0.2094E-02	0.1116E+00	0.6694E+09	252.7159	0.3120E+00	0.5138E-05	211.3305	0.1420E-05
73000.00	0.2109E-02	0.1251E+00	0.7378E+09	260.0000	0.3384E+00	0.5545E-05	212.3080	0.1425E-05
72500.00	0.2122E-02	0.1387E+00	0.8272E+09	262.5000	0.3648E+00	0.5953E-05	213.2855	0.1431E-05
72000.00	0.2135E-02	0.1527E+00	0.9320E+09	265.0000	0.3912E+00	0.6360E-05	214.2630	0.1436E-05
71500.00	0.2154E-02	0.1715E+00	0.1032E+10	265.0000	0.4265E+00	0.6882E-05	215.5935	0.1444E-05
71000.00	0.2171E-02	0.1908E+00	0.1147E+10	265.0000	0.4618E+00	0.7403E-05	216.9240	0.1451E-05
70500.00	0.2188E-02	0.2105E+00	0.1278E+10	262.5000	0.4971E+00	0.7925E-05	218.2545	0.1459E-05
70000.00	0.2216E-02	0.2360E+00	0.1439E+10	260.0000	0.5608E+00	0.8668E-05	219.5850	0.1501E-05
69500.00	0.2237E-02	0.2568E+00	0.1581E+10	253.2735	0.6067E+00	0.9178E-05	220.9550	0.1518E-05
69000.00	0.2256E-02	0.2777E+00	0.1744E+10	247.2294	0.6526E+00	0.9687E-05	222.3250	0.1535E-05
68500.00	0.2274E-02	0.3019E+00	0.1937E+10	243.6616	0.6985E+00	0.1030E-04	223.6950	0.1548E-05
68000.00	0.2291E-02	0.3264E+00	0.2161E+10	239.7943	0.7444E+00	0.1091E-04	225.0650	0.1562E-05
67500.00	0.2313E-02	0.3573E+00	0.2378E+10	235.0475	0.8005E+00	0.1162E-04	226.4360	0.1573E-05
67000.00	0.2333E-02	0.3887E+00	0.2626E+10	229.9371	0.8565E+00	0.1234E-04	227.8070	0.1585E-05
66500.00	0.2359E-02	0.4254E+00	0.2918E+10	224.1746	0.9228E+00	0.1310E-04	229.1780	0.1596E-05
66000.00	0.2383E-02	0.4627E+00	0.3256E+10	218.3462	0.9891E+00	0.1387E-04	230.5490	0.1607E-05
65500.00	0.2405E-02	0.5061E+00	0.3578E+10	211.9359	0.1055E+01	0.1479E-04	231.9208	0.1614E-05
65000.00	0.2426E-02	0.5502E+00	0.3946E+10	204.5884	0.1122E+01	0.1570E-04	233.2925	0.1621E-05
64500.00	0.2453E-02	0.6093E+00	0.4382E+10	195.7500	0.1203E+01	0.1683E-04	234.6643	0.1623E-05
64000.00	0.2479E-02	0.6701E+00	0.4885E+10	186.9316	0.1285E+01	0.1795E-04	236.0360	0.1625E-05
63500.00	0.2508E-02	0.7424E+00	0.5383E+10	180.0917	0.1377E+01	0.1922E-04	237.4088	0.1625E-05
63000.00	0.2536E-02	0.8171E+00	0.5952E+10	173.2910	0.1468E+01	0.2050E-04	238.7815	0.1625E-05
62500.00	0.2567E-02	0.9063E+00	0.6619E+10	166.5228	0.1575E+01	0.2197E-04	240.1543	0.1626E-05
62000.00	0.2598E-02	0.9983E+00	0.7387E+10	159.9759	0.1683E+01	0.2345E-04	241.5270	0.1627E-05
61500.00	0.2631E-02	0.1107E+01	0.8155E+10	154.4100	0.1805E+01	0.2514E-04	242.9005	0.1627E-05

61000.00	0.2664E-02	0.1219E+01	0.9021E+10	148.8325	0.1927E+01	0.2682E-04	244.2740	0.1628E-05
60500.00	0.2699E-02	0.1350E+01	0.1004E+11	142.8504	0.2065E+01	0.2876E-04	245.6475	0.1629E-05
60000.00	0.2732E-02	0.1485E+01	0.1120E+11	136.9296	0.2203E+01	0.3069E-04	247.0210	0.1630E-05
59500.00	0.2769E-02	0.1623E+01	0.1237E+11	133.7313	0.2361E+01	0.3263E-04	248.3953	0.1639E-05
59000.00	0.2805E-02	0.1762E+01	0.1368E+11	130.2026	0.2519E+01	0.3457E-04	249.7695	0.1648E-05
58500.00	0.2843E-02	0.1925E+01	0.1575E+11	124.7408	0.2692E+01	0.3676E-04	251.1438	0.1656E-05
58000.00	0.2879E-02	0.2091E+01	0.1817E+11	119.4967	0.2865E+01	0.3895E-04	252.5180	0.1663E-05
57500.00	0.2919E-02	0.2287E+01	0.2073E+11	115.6835	0.3064E+01	0.4145E-04	253.8933	0.1670E-05
57000.00	0.2958E-02	0.2486E+01	0.2363E+11	111.8781	0.3263E+01	0.4395E-04	255.2685	0.1676E-05
56500.00	0.3002E-02	0.2739E+01	0.2711E+11	108.2920	0.3492E+01	0.4691E-04	256.6438	0.1679E-05
56000.00	0.3045E-02	0.2996E+01	0.3110E+11	104.7598	0.3722E+01	0.4986E-04	258.0190	0.1681E-05
55500.00	0.3091E-02	0.3319E+01	0.3527E+11	101.8301	0.3977E+01	0.5343E-04	259.3953	0.1678E-05
55000.00	0.3135E-02	0.3655E+01	0.3998E+11	98.8576	0.4232E+01	0.5700E-04	260.7715	0.1676E-05
54500.00	0.3184E-02	0.4022E+01	0.4556E+11	94.6691	0.4527E+01	0.6088E-04	262.1478	0.1678E-05
54000.00	0.3231E-02	0.4400E+01	0.5196E+11	90.6477	0.4823E+01	0.6475E-04	263.5240	0.1680E-05
53500.00	0.3282E-02	0.4824E+01	0.5870E+11	87.8068	0.5155E+01	0.6898E-04	264.9008	0.1684E-05
53000.00	0.3331E-02	0.5257E+01	0.6627E+11	84.9696	0.5486E+01	0.7322E-04	266.2775	0.1688E-05
52500.00	0.3384E-02	0.5764E+01	0.7608E+11	82.4393	0.5858E+01	0.7806E-04	267.6543	0.1691E-05
52000.00	0.3434E-02	0.6281E+01	0.8806E+11	79.9429	0.6230E+01	0.8290E-04	269.0310	0.1695E-05
51500.00	0.3490E-02	0.6890E+01	0.1010E+12	78.3556	0.6659E+01	0.8836E-04	269.4358	0.1698E-05
51000.00	0.3545E-02	0.7518E+01	0.1163E+12	76.5063	0.7087E+01	0.9381E-04	269.8405	0.1701E-05
50500.00	0.3603E-02	0.8249E+01	0.1347E+12	73.1246	0.7566E+01	0.1001E-03	270.2453	0.1702E-05
50000.00	0.3659E-02	0.9004E+01	0.1560E+12	69.8879	0.8045E+01	0.1064E-03	270.6500	0.1703E-05
49500.00	0.3722E-02	0.9978E+01	0.1791E+12	68.4122	0.8596E+01	0.1140E-03	270.6500	0.1699E-05
49000.00	0.3782E-02	0.1097E+02	0.2054E+12	66.9365	0.9147E+01	0.1217E-03	270.6500	0.1694E-05
48500.00	0.3847E-02	0.1214E+02	0.2358E+12	65.4609	0.9774E+01	0.1304E-03	270.6500	0.1691E-05
48000.00	0.3910E-02	0.1335E+02	0.2742E+12	63.9796	0.1040E+02	0.1392E-03	270.6500	0.1687E-05
47500.00	0.3978E-02	0.1460E+02	0.3196E+12	61.9409	0.1112E+02	0.1482E-03	269.7188	0.1691E-05
47000.00	0.4043E-02	0.1587E+02	0.3715E+12	59.9021	0.1184E+02	0.1572E-03	268.7875	0.1696E-05
46500.00	0.4113E-02	0.1731E+02	0.4320E+12	57.8634	0.1264E+02	0.1672E-03	267.8563	0.1701E-05
46000.00	0.4179E-02	0.1877E+02	0.5058E+12	55.8248	0.1345E+02	0.1772E-03	266.9250	0.1706E-05
45500.00	0.4252E-02	0.2072E+02	0.5948E+12	53.7882	0.1436E+02	0.1899E-03	265.5445	0.1702E-05
45000.00	0.3586E-02	0.1933E+02	0.5786E+12	51.7515	0.1528E+02	0.2025E-03	264.1640	0.1698E-05
44500.00	0.3165E-02	0.1890E+02	0.5890E+12	49.7269	0.1633E+02	0.2175E-03	262.7835	0.1692E-05
44000.00	0.2887E-02	0.1891E+02	0.6235E+12	47.7763	0.1738E+02	0.2325E-03	261.4030	0.1685E-05
43500.00	0.2717E-02	0.1955E+02	0.6712E+12	46.1620	0.1858E+02	0.2499E-03	260.0218	0.1679E-05
43000.00	0.2594E-02	0.2036E+02	0.7405E+12	44.7700	0.1979E+02	0.2674E-03	258.6405	0.1672E-05
42500.00	0.2468E-02	0.2112E+02	0.8139E+12	43.3781	0.2117E+02	0.2865E-03	257.2593	0.1670E-05
42000.00	0.1708E-02	0.2189E+02	0.6451E+12	41.9773	0.2256E+02	0.3056E-03	255.8780	0.1667E-05
41500.00	0.1585E-02	0.2181E+02	0.6623E+12	39.7103	0.2414E+02	0.3277E-03	254.4960	0.1665E-05
41000.00	0.1471E-02	0.2166E+02	0.6825E+12	37.4433	0.2573E+02	0.3499E-03	253.1140	0.1662E-05
40500.00	0.1378E-02	0.2201E+02	0.7182E+12	35.1763	0.2755E+02	0.3774E-03	251.7320	0.1653E-05

40000.00	0.1271E-02	0.2189E+02	0.7499E+12	32.9893	0.2937E+02	0.4049E-03	250.3500	0.1644E-05
39500.00	0.1299E-02	0.2429E+02	0.8229E+12	32.7221	0.3148E+02	0.4372E-03	248.9670	0.1635E-05
39000.00	0.1325E-02	0.2673E+02	0.8893E+12	32.4548	0.3359E+02	0.4695E-03	247.5840	0.1626E-05
38500.00	0.1353E-02	0.2969E+02	0.9683E+12	32.1876	0.3604E+02	0.5075E-03	246.2010	0.1617E-05
38000.00	0.1352E-02	0.3206E+02	0.1037E+13	31.4934	0.3849E+02	0.5454E-03	244.8180	0.1608E-05
37500.00	0.1281E-02	0.3305E+02	0.1049E+13	29.7936	0.4135E+02	0.5903E-03	243.4340	0.1599E-05
37000.00	0.1221E-02	0.3410E+02	0.1077E+13	28.0937	0.4420E+02	0.6352E-03	242.0500	0.1590E-05
36500.00	0.1136E-02	0.3457E+02	0.1085E+13	26.3939	0.4753E+02	0.6882E-03	240.6660	0.1581E-05
36000.00	0.1080E-02	0.3560E+02	0.1125E+13	24.9562	0.5085E+02	0.7412E-03	239.2820	0.1572E-05
35500.00	0.1100E-02	0.3956E+02	0.1230E+13	24.7132	0.5474E+02	0.8039E-03	237.8973	0.1564E-05
35000.00	0.1116E-02	0.4351E+02	0.1347E+13	24.4701	0.5863E+02	0.8667E-03	236.5125	0.1555E-05
34500.00	0.1132E-02	0.4770E+02	0.1482E+13	24.2270	0.6316E+02	0.9356E-03	235.1278	0.1552E-05
34000.00	0.1141E-02	0.5174E+02	0.1634E+13	23.9345	0.6768E+02	0.1005E-02	233.7430	0.1549E-05
33500.00	0.1108E-02	0.5479E+02	0.1706E+13	22.9427	0.7295E+02	0.1090E-02	232.4298	0.1541E-05
33000.00	0.1077E-02	0.5774E+02	0.1794E+13	21.9509	0.7823E+02	0.1175E-02	231.1165	0.1533E-05
32500.00	0.1042E-02	0.6060E+02	0.1888E+13	20.9591	0.8439E+02	0.1272E-02	229.8033	0.1529E-05
32000.00	0.9924E-03	0.6225E+02	0.1971E+13	19.9673	0.9054E+02	0.1368E-02	228.4900	0.1525E-05
31500.00	0.9515E-03	0.6425E+02	0.2028E+13	18.9755	0.9768E+02	0.1474E-02	227.9948	0.1527E-05
31000.00	0.9084E-03	0.6569E+02	0.2090E+13	17.9836	0.1048E+03	0.1580E-02	227.4995	0.1528E-05
30500.00	0.8602E-03	0.6802E+02	0.2147E+13	16.9918	0.1131E+03	0.1719E-02	227.0043	0.1520E-05
30000.00	0.8190E-03	0.7036E+02	0.2234E+13	16.0000	0.1215E+03	0.1857E-02	226.5090	0.1511E-05
29500.00	0.8120E-03	0.7590E+02	0.2382E+13	15.4951	0.1312E+03	0.2014E-02	226.0135	0.1507E-05
29000.00	0.8061E-03	0.8148E+02	0.2556E+13	14.9902	0.1410E+03	0.2172E-02	225.5180	0.1502E-05
28500.00	0.7892E-03	0.8820E+02	0.2578E+13	14.4852	0.1525E+03	0.2380E-02	225.0225	0.1489E-05
28000.00	0.7677E-03	0.9415E+02	0.2673E+13	13.9803	0.1640E+03	0.2587E-02	224.5270	0.1475E-05
27500.00	0.7451E-03	0.9934E+02	0.2899E+13	13.4754	0.1776E+03	0.2808E-02	224.0313	0.1473E-05
27000.00	0.7233E-03	0.1042E+03	0.3122E+13	12.9705	0.1913E+03	0.3028E-02	223.5355	0.1470E-05
26500.00	0.7086E-03	0.1110E+03	0.3236E+13	12.4655	0.2072E+03	0.3288E-02	223.0398	0.1468E-05
26000.00	0.6934E-03	0.1174E+03	0.3370E+13	11.9617	0.2231E+03	0.3547E-02	222.5440	0.1466E-05
25500.00	0.6675E-03	0.1229E+03	0.3365E+13	11.4703	0.2418E+03	0.3852E-02	222.0480	0.1463E-05
25000.00	0.6356E-03	0.1265E+03	0.3367E+13	10.9789	0.2605E+03	0.4158E-02	221.5520	0.1460E-05
24500.00	0.6058E-03	0.1282E+03	0.3390E+13	10.4875	0.2831E+03	0.4463E-02	221.0560	0.1474E-05
24000.00	0.5830E-03	0.1326E+03	0.3469E+13	9.9960	0.3030E+03	0.4786E-02	220.5600	0.1471E-05
23500.00	0.5675E-03	0.1414E+03	0.3405E+13	9.4919	0.3304E+03	0.5234E-02	220.0635	0.1469E-05
23000.00	0.5518E-03	0.1496E+03	0.3256E+13	8.9879	0.3579E+03	0.5682E-02	219.5670	0.1466E-05
22500.00	0.5194E-03	0.1522E+03	0.2593E+13	8.4839	0.3853E+03	0.6130E-02	219.0705	0.1463E-05
22000.00	0.4673E-03	0.1472E+03	0.2533E+13	7.9898	0.4127E+03	0.6578E-02	218.5740	0.1460E-05

EI=001.33

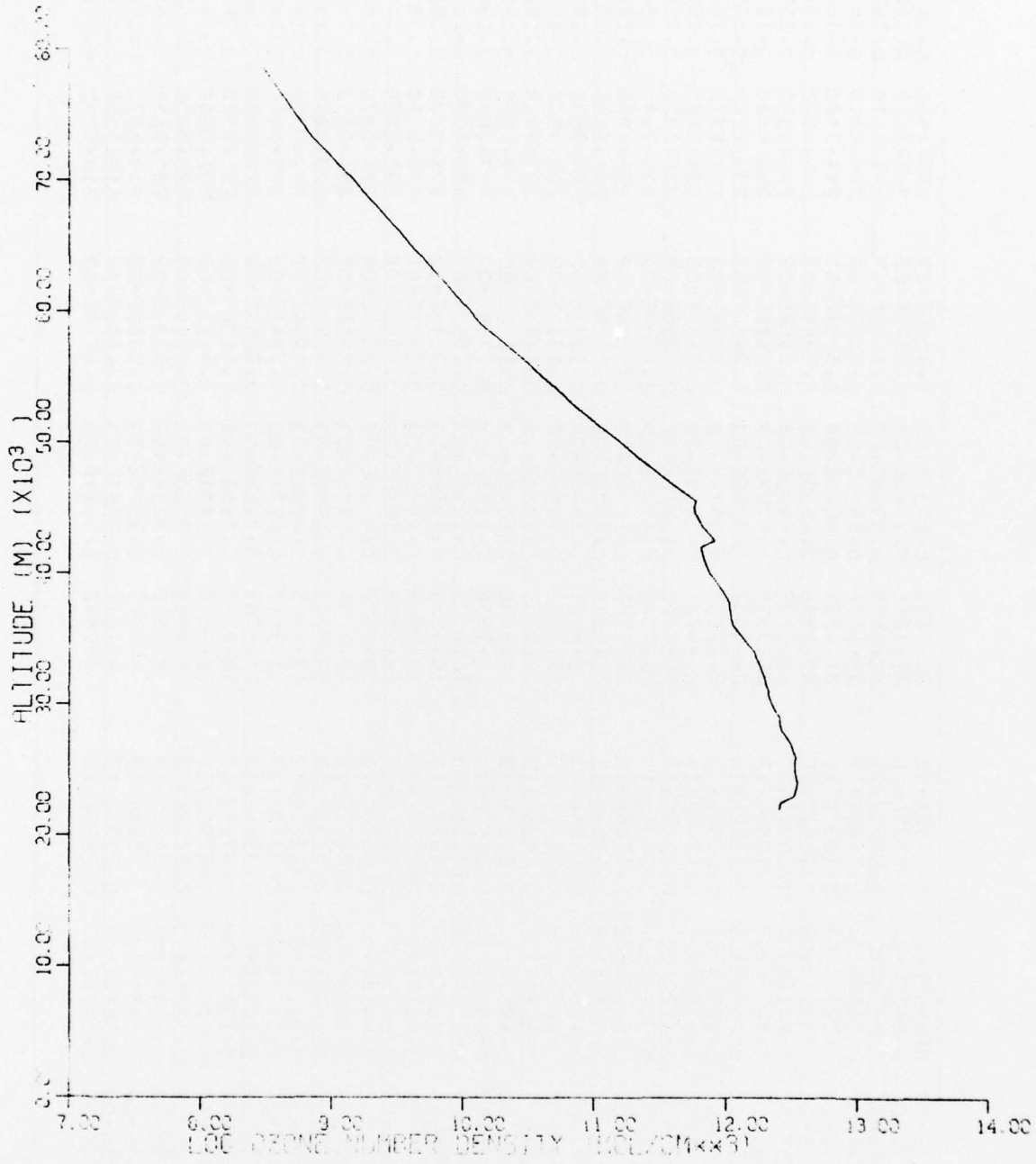

☆ U.S. GOVERNMENT PRINTING OFFICE: 1977 777-093/51